JOC The Journal of Organic Chemistry

pubs.acs.org/joc Article

Synthesis of 3-Carbonyl Trisubstituted Furans via Pd-Catalyzed Aerobic Cycloisomerization Reaction: Development and Mechanistic Studies

Amanda A. Barboza,[§] Attilio Chiavegatti Neto,[§] Isac G. Rosset, Guilherme A. M. Jardim, and Marco A. B. Ferreira*

Cite This: J. Org. Chem. 2021, 86, 3923−3942 Read Online

ACCESS | Metrics & More | Article Recommendations | Supporting Information

ABSTRACT: Herein, we report the synthesis of 3-carbonyl-trisubstituted furans via Pd-catalyzed oxidative cycloisomerization reactions of 2-alkenyl-1,3-dicarbonyl scaffolds, using molecular oxygen as the sole oxidant to regenerate active palladium catalytic species, featuring good functional tolerance and mild reaction conditions. Deep investigation of intermediates and transition states of the reaction mechanism were conducted via experimental and DFT studies, providing a detailed mechanistical profile. The new developed methodology presents a greener alternative to Wacker-type cycloisomerizations and avoids the use of stoichiometric amounts of oxidants and strong acid additives.

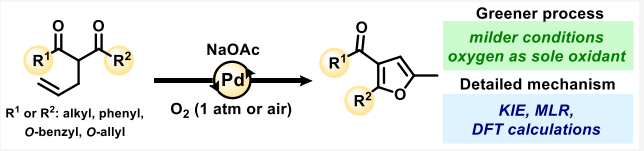

INTRODUCTION

Furans represent an important class of electron-rich five-membered heterocyclic compounds, which are broadly distributed as structural frameworks in natural products[1] and biologically relevant moieties, including important pharmaceutical ingredients.[2] Remarkably, 3-carbonyl-bearing furans are a common occurrence in current drug prototypes, such as amiodarone,[3] sarcofuranocembrenolide B,[4] and wortmannin,[5] considered important examples of bioactive molecules (Figure 1). In 2017, Dong and co-workers reported the synthesis and antiviral activity against lethal H5N1 influenza A viruses of unprecedented furan-carboxamide derivatives (Figure 1).[6] In the past few decades, transition-metal-catalyzed reactions involving oxygen atoms and nonactivated π-bonds comprised the strategy of choice to synthesize polysubstituted furans.[7] Palladium-catalyzed reactions embody some of the most powerful methods for selective oxidative intramolecular cycloisomerization strategies,[8,9] but at the end of the process, generated Pd^0 requires the use of a stoichiometric oxidant, such as Cu^{II}, Ag^{I}, benzoquinone, or O_2 to regenerate Pd^{II} species.[10]

The use of stoichiometric amounts of molecular oxygen as reoxidant, allied with catalytic amounts of palladium complexes, has enormous advantages due to the sustainability associated with the formation of environmentally benign byproducts like water and hydrogen peroxide.[11] However, in the absence of a cocatalyst, Pd^0 has a tendency to precipitate into its inactive metallic form.[12,13] In some cases, improved stability of Pd^0-based catalysts is observed in the presence of molecular sieves[14] and ancillary ligands.[15] In this context, current research has focused on the development of more environmentally friendly methods in order to avoid the use of these oxidants,[16] and several Pd^{II} catalyzed aerobic oxidative transformations were highlighted in recent reviews.[9,11,13] An important example comprises the aerobic oxidations of alcohols mediated by Pd^{II} chiral diamines by Sigman and co-workers (Scheme 1A).[17] For aerobic asymmetric cyclizations, the unprecedented work of Stoltz and collaborators describes the synthesis of substituted benzofuran moieties in excellent yields and stereoselectivity (Scheme 1B).[18] Among Pd-catalyzed intramolecular cycloisomerization methodologies to form 3-carbonyl furans, the use of 2-alkynyl-1,3-dicarbonyl substrates had received considerable attention from the synthetic community.[19] Curiously, although 2-alkenyl-1,3-dicarbonyl-based compounds are the most structurally accessible substrates, they were barely explored in the context of Wacker-type chemistry to access these frameworks. To date, only two methodologies were found in literature regarding the Pd-catalyzed aerobic synthesis of 3-carbonyl trisubstituted furans. The pioneering work described by Han and Widenhoefer presents a limited scope and the need for an excessive amount of $CuCl_2$ cooxidant for catalyst regeneration.[20] In subsequent works, Ghorai and co-workers demonstrated the synthesis of polysubstituted furans and the oxidative cyclization of *o*-cinnamyl phenols through the use of substituted olefins.[21] However, both reactions requires the use

Received: November 19, 2020
Published: February 24, 2021

https://dx.doi.org/10.1021/acs.joc.0c02777
J. Org. Chem. 2021, 86, 3923−3942

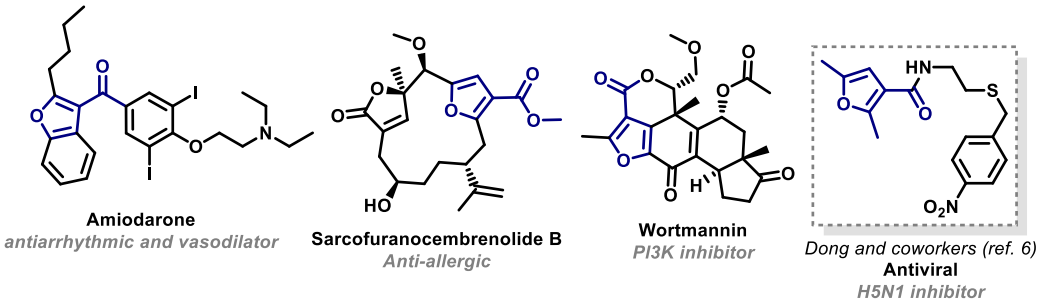

Figure 1. Examples of occurrence of substituted furans in natural products and drug prototypes.

Scheme 1. Summary of Previous Methodologies and Work overview

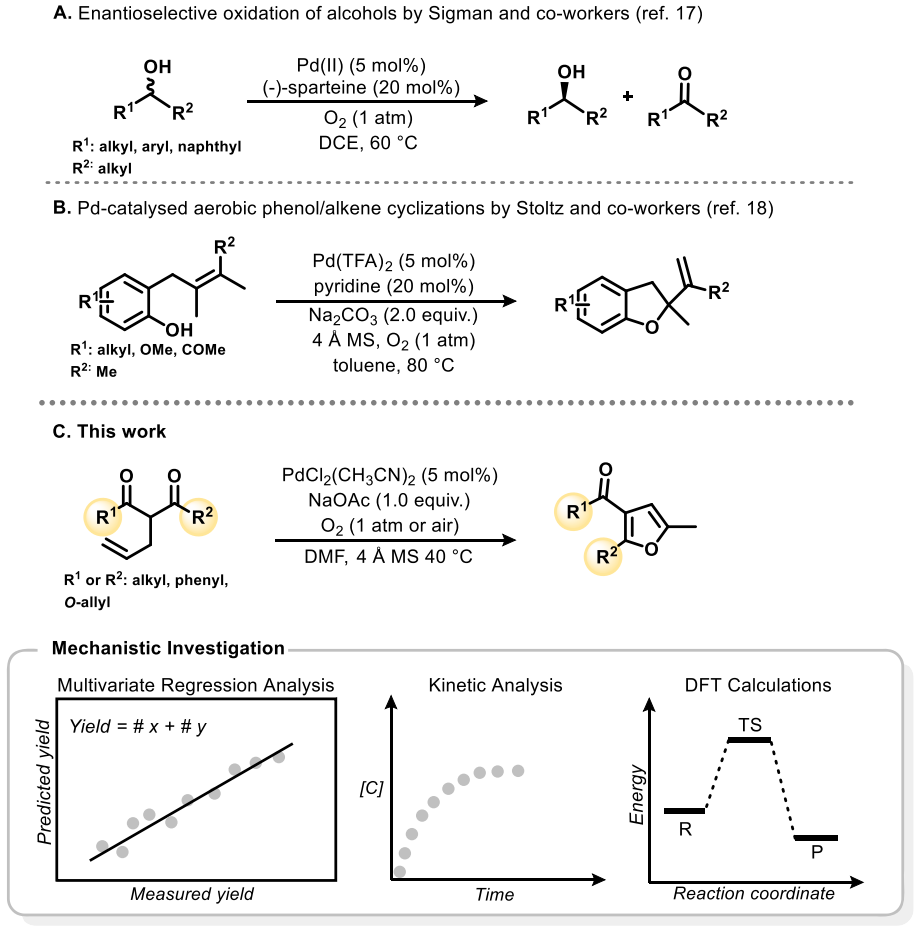

of stoichiometric quantities of benzoquinone as oxidant and/or strong acid (*p*-TsOH) as additive. As part of our interest in metal-catalyzed aerobic oxidative processes,[22] herein we describe the development, scope, and limitations in the synthesis of 3-carbonyl trisubstituted furans via Pd-catalyzed oxidative cycloisomerization reactions of 2-alkenyl-1,3-dicarbonyl compounds, using molecular oxygen as the sole oxidant to regenerate active palladium catalyst species (Scheme 1C). We also propose a mechanistic rationalization supported by DFT calculations, NMR experiments, multivariate regression analysis, and kinetic isotopic effects (KIE) of this transformation.

RESULTS AND DISCUSSION

Based on a previous report relating the promotion of the Pd-mediated aerobic heterocyclization reactions in basic medium using K_2CO_3,[18] we started our investigation about the reactivity of 2-alkenyl-*β*-ketoester **1a** by exploring similar related conditions, using 5 mol % of $PdCl_2(CH_3CN)_2$ as catalyst in DMF (entry 1, Table 1). This preliminary experiment led to complete consumption of the starting material, but a low yield of **2a** was observed, together with a complex mixture of byproducts. No further improvement was obtained by decreasing the reaction temperature to 40 °C (entry 2). Next, use of NaOAc resulted in 60% yield of the expected furan (entry 3), while the use of a bulkier and stronger base (*t*-BuOK, entry 4) led to inhibition of the desired product. The effect of the base stoichiometry (entries 5−7) and temperature variation (entries 8−9) were also evaluated, but no improvement in yield was observed. The choice of Pd^{II} source was found to impact catalytic efficiency (entry 3 versus entries 11−15), but the investigated options provided

https://dx.doi.org/10.1021/acs.joc.0c02777
J. Org. Chem. 2021, 86, 3923−3942

Table 1. Optimization of the Reaction Conditions for the formation of 2a*

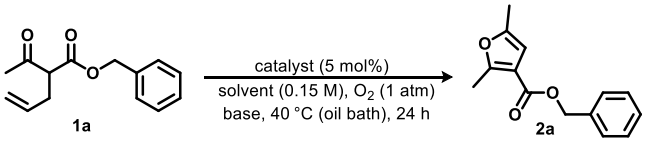

entry	catalyst	base (equiv)	solvent	yield (%)
1[a]	$Pd(CH_3CN)_2Cl_2$	K_2CO_3(1.0)	DMF	16
2	$Pd(CH_3CN)_2Cl_2$	K_2C0_3(1.0)	DMF	12
3	$Pd(CH_3CN)_2Cl_2$	NaOAc (1.0)	DMF	60
4	$Pd(CH_3CN)_2Cl_2$	^{t}BuOK (1.0)	DMF	NR
5	$Pd(CH_3CN)_2Cl_2$	NaOAc (2.0)	DMF	60
6	$Pd(CH_3CN)_2Cl_2$	NaOAc (0.2)	DMF	50
7	$Pd(CH_3CN)_2Cl_2$	-	DMF	17
8[b]	$Pd(CH_3CN)_2Cl_2$	NaOAc (1.0)	DMF	33
9[c]	$Pd(CH_3CN)_2Cl_2$	NaOAc (1.0)	DMF	42
10	$Pd(C_6H_3CN)_2Cl_2$	NaOAc (1.0)	DMF	43
11	$PdCl_2$	NaOAc (1.0)	DMF	43
12	$Pd(OAc)_2$	NaOAc (1.0)	DMF	20
13	$Pd(TFA)_2$	NaOAc (1.0)	DMF	20
14	$Pd(Phen)Cl_2$	NaOAc (1.0)	DMF	NR
15	$Pd(Quinox)Cl_2$	NaOAc (1.0)	DMF	12
16[d]	$Pd(CH_3CN)_2Cl_2$	NaOAc (1.0)	DMF	27
17	$Pd(CH_3CN)_2Cl2$	NaOAc (1.0)	dioxane	23
18	$Pd(CH_3CN)_2Cl_2$	NaOAc (1.0)	THF	27
19	$Pd(CH_3CN)_2Cl_2$	NaOAc (1.0)	DMAc	38
20	$Pd(CH_3CN)_2Cl_2$	NaOAc (1.0)	DMSO	NR
21	$Pd(CH_3CN)_2Cl_2$	NaOAc (1.0)	acetonitrile	6
22	$Pd(CH_3CN)_2Cl_2$	NaOAc (1.0)	PEG 400	15
23	$Pd(CH_3CN)_2Cl_2$	NaOAc (1.0)	toluene	13
24	$Pd(CH_3CN)_2Cl_2$	NaOAc (1.0)	anisole	3
25[e]	**$Pd(CH_3CN)_2Cl_2$**	**NaOAc (1.0)**	**DMF**	**70**
26[f]	$Pd(CH_3CN)_2Cl_2$	NaOAc (1.0)	DMF	62

*The tests were performed employing 0.3 mmol of **1a** in 2 mL of solvent and O_2 atmosphere (1 atm). Variations in reaction conditions are described in each footnote. [a]80 °C and 0.1 M. [b]60 °C. [c]rt. [d]2.5 mol % of $Pd(CH_3CN)_2Cl_2$. [e]80 mg of 4 Å molecular sieves. [f]Addition of LiCl (1.0 equiv).

unsatisfactory results. When 2.5 mol % of $PdCl_2(CH_3CN)_2$ was used, **2a** was obtained in only 27% yield (entry 16). A brief examination of the effects of solvents showed that the use of polar solvents resulted in poorer reaction performance. The use of dioxane, THF, DMAc, and toluene in place of DMF afforded low yields (entries 17−20), while DMSO and acetonitrile (entries 20 and 21) were considerably less effective. Green solvents such as PEG 400 and anisole (entries 22 and 24) were also tested, showing equal inefficiency. Finally, use of 4 Å molecular sieves provided the desired product in 70% yield (entry 25), and use of a halogenated additive (LiCl) resulted in a slight decrease in yield (entry 26).

After establishing the best reactional parameters (entry 25, Table 1), our efforts continued to provide a scope for the optimized transformation. The first modification was carried out on the ester portion of 1,3-dicarbonyl substrates (Scheme 2). Substitution patterns on the aryl group by electron-donating and -withdrawing groups displayed average variations in yield (**2a**−**e**). Although reaction with an electron donor *p*-OMe substituent (**2b**, 70% yield) showed no apparent effect, electron-withdrawing substituents (**2c**−**e**) resulted in decreases in yield, with complete conversion of starting materials. in

Scheme 2. Scope for Pd-Catalyzed Aerobic Cycloisomerization of 1,3-Dicabonyl Ester Derivatives Bearing O-Substituents*

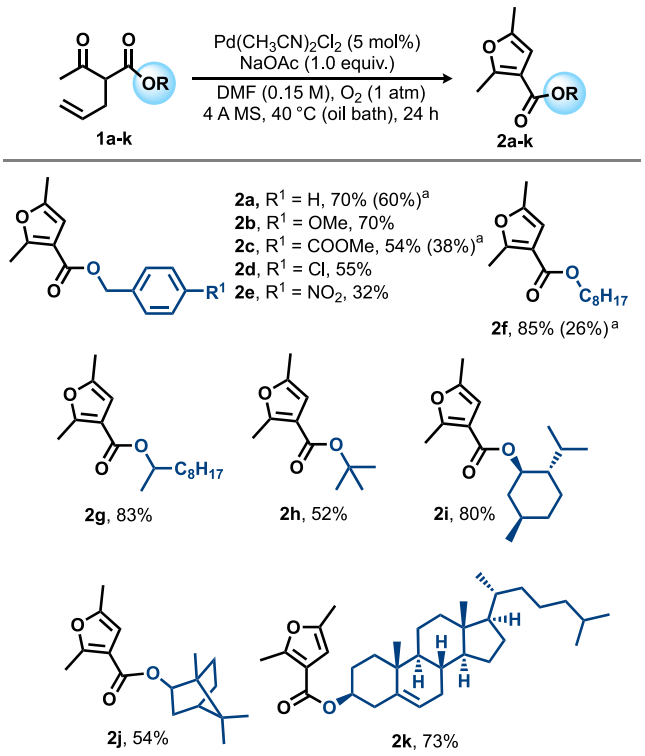

*Isolated yields are shown. [a]Without 4 A MS.

particular, *p*-NO_2 benzylic substrate (**1e**) gave **2e** in only 32% yield. Analysis by GC−MS (Figure S1) showed the presence of benzyl alcohol, potentially from ester hydrolysis of **2a** in which this result could partially explain the lower yield involving electron-withdrawing ester substituents. In general, reactions with different substrates were monitored via TLC and total starting material consumption was observed after 24 h. It was noted that longer reaction times provided minor yields in several cases, even when starting material was still detected.

Overall, the yields were usually lower when bulkier ester moieties were employed (**2f**−**j**), possibly due to hindering effects at cyclization steps. Primary and secondary alkyl esters afforded high yields (**2f**−**g**,**i**, >80% yield), except for the sterically bulky isoborneol derivative **1j** (**2j**, 54% yield), showing similar results with tertiary alkyl ester **1h** (**2h**, 52% yield). When the structural complexity was increased, such as the introduction of a cholesterol backbone, a satisfactory yield of 73% was observed for **2k**. The importance of molecular sieves was evaluated for representative substrates **2a**,**c**,**f** (yields in parentheses, Scheme 2), highlighting how the reaction performance is dramatically affected by this additive.

Next, we explored possibilities of modification in the ketone portion of *β*-ketoester substrates (**4a**−**h**) (Scheme 3). Evaluating the electronic demand of aromatic groups (**4a**−**c**), a small decrease in yield was observed in the presence of an electron-withdrawing nitro group (**4b**). It was noted that longer reaction times provided minor yields, as exemplified for products **4a** and **4b**, which provided yields of 52% and 38%, respectively, after 40 h of reaction. A variety of alkyl chains, such as the ethyl (**4d**), isopropyl (**4e**), and cyclopropyl (**4f**) at the ketone portion, were compatible, providing average to

https://dx.doi.org/10.1021/acs.joc.0c02777
J. Org. Chem. 2021, 86, 3923−3942

Scheme 3. Scope for Pd-Catalyzed Aerobic Cycloisomerization of 1,3-Dicarbonyl Ketone Derivatives Bearing Different Groups in the Ketone Portion*

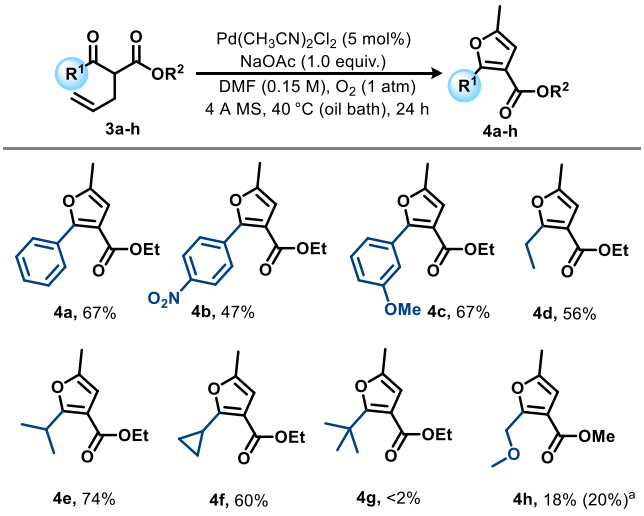

*Isolated yields. [a]Addition of LiCl (1 equiv).

good yields, where **4d** proved to be volatile, which explains a decrease in yield. As expected, the *tert*-butyl derivative suppressed the formation of products, providing **4g** with less than 2% yield, reflecting the severe steric hindrance imposed by this substituent. When a methoxymethyl side chain substrate was employed, the desired product **4h** was obtained in low yields (18% and 20% with addition of LiCl), potentially due to the formation of bidentate complex palladium species.[23] In general, lower yields could be attributed to ester group decomposition (further details are discussed in the Parametrization and Multivariate Regression Analysis section).

Finally, to determine the generality of the cyclization, substituted β-diketone substrates **5a−e** were investigated (Scheme 4). The optimized established conditions enabled the use of nonsymmetric acyclic diketone (**5a**), giving **6a** in 50% yield and complete regioselectivity. The symmetrical

Scheme 4. Scope for More Challenging Substrates[a]

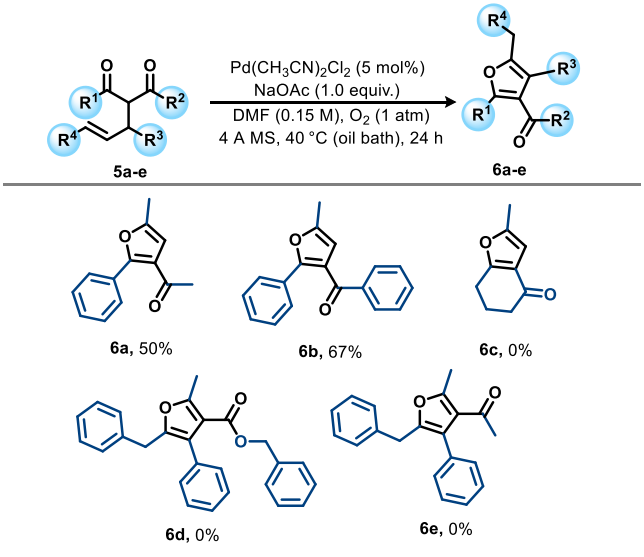

[a]Isolated yields.

substrate **5b** provided derivative **6b** in 67% yield. Unfortunately, for cyclic β-diketone **5c** and tetrasubstituted substrates **5d−e**, the optimized protocol was not sufficient to promote cyclization.

To evaluate the effect of molecular oxygen in the reaction processing, a control experiment with system deoxygenation was performed using the freeze−pump−thaw deoxygenation technique,[24] resulting in 15% yield of **2a**, while the absence of molecular sieves furnished the same product in 4% yield (Scheme 5A). This fact may be due to remaining O_2 being

Scheme 5. Control Experiments and Scaling Effects for the Optimized Conditions

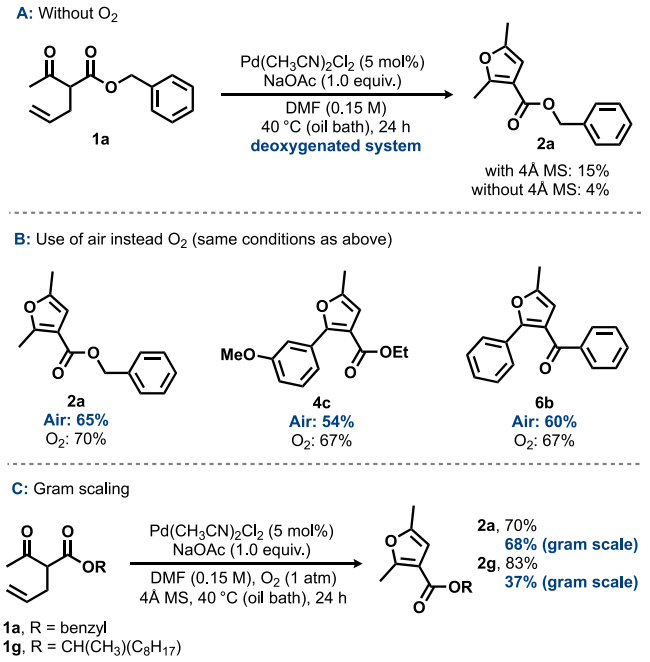

strongly adsorbed on the molecular sieves. These yields are considerably lower than those obtained under the optimized conditions, corroborating the importance of oxygen in reactional media. Additionally, the use of atmospheric air as a source of oxygen was evaluated for substrates **1a**, **3c**, and **5b** (Scheme 5B). It was observed that reaction was efficient, and yields for derivatives **2a**, **4c**, and **6b** were close to the ones obtained using the optimized condition. These results show that the reactions can be performed in order to avoid the use of oxygen gas, increasing the safety of procedures at the cost of a small loss of performance. In terms of applicability, the reaction was escalated to gram scale, resulting in product **2a** with 68% yield (Scheme 5C).

MECHANISTIC INVESTIGATION

Initial Considerations. Nucleopalladations are considered one of the most common mechanisms for palladium-catalyzed oxidative functionalization of olefins, where the formation of π-alkene−palladium complexes plays a fundamental role in stereo- and regioselectivity.[25] The interactions between a nucleophile and the π-bond of palladated intermediates are governed by a combination of steric and electronic effects, such as orbital interactions,[26] steric bulky of involved species,[27] dispersion forces, and electrostatics.[28] Recently, Liu and co-workers analyzed these different types of nucleophile−substrate interactions using a computational approach.[29] The

https://dx.doi.org/10.1021/acs.joc.0c02777
J. Org. Chem. 2021, 86, 3923−3942

Scheme 6. Possibilities for Reaction Pathways Investigated in This Work

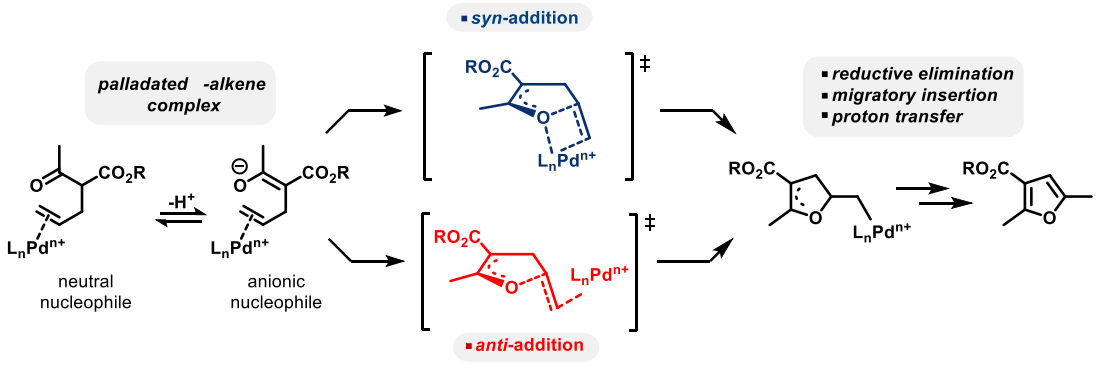

electronic nature of palladium catalysts, controlled by anionic coordinated ligand additives,[30] can alter the polarization of the electron-density of olefins in the palladated π-alkene complex, and together with the analysis of the nucleophile, it is possible to predict Markovnikov selectivity in the transition states as well as plausible intermediates in intermolecular nucleopalladation processes.

Considered equally important, palladium-catalyzed stereocontrolled intramolecular nucleophilic attacks on metal coordinated olefins[31] using oxygen[32] or nitrogen[33] atoms as nucleophiles have been heavily investigated in the literature. Insightful examples can be found in the works of Wolfe[34] and Stahl.[35] Intramolecular Wacker-type oxidative cyclizations, after the oxypalladation step, can proceed by a most favorable 5-*exo*-cyclization, with two possibilities of attack (*anti* and *syn*).[36] Previous works showed that strongly and bulky coordinated ligands at Pd core like Cl^- favors *anti*-oxypalladation by hindering the nucleophile attack,[37] while use of nonmetal oxidants like molecular oxygen or benzoquinone, in the absence of salt additives, makes *syn*-oxypalladation addition more favorable.[38,39] Despite this knowledge, there is a lack of works aimed at the understanding of the main steps of the mechanism of 2-alkenyl-1,3-dicarbonyl scaffolds in palladium cycloisomerizations, and the study of such a process is essential. In this section, we disclose a full mechanistic rationalization supported by DFT calculations, NMR experiments, multivariate regression analysis, and KIE experiments (Scheme 6).

NMR and KIE Experiments. The use of a base for the reaction follows the hypothesis that the oxo-palladation step is preceded by a tautomerization equilibrium, and the enolic form would be responsible for the attack.[21] Following this hypothesis, NMR studies were conducted (see the Supporting Information, section 4), revealing no α-carbonyl proton abstraction in **1a** after base addition. Additionally, we observe an absence of deprotonated substrate after addition of $PdCl_2(CH_3CN)_2$. These results may indicate no accumulation of this active specie in reaction media and, therefore, the involvement of the α-carbonyl proton removal in the rate-determining step of the process. To support this hypothesis, kinetic isotopic effect (KIE) experiments were conducted (Scheme 7 and Supporting Information) resulting in a k_H/k_D = 1.70 ± 0.14, suggesting a rate-limiting step related to the α-carbonyl proton removal by NaOAc.

DFT Calculations. Mechanistic description based on theoretical methods regarding intramolecular oxypalladations were thoroughly investigated for alkenol-based substrates.[40] Until recently, mechanistic interpretations based on computational studies involving Pd-catalyzed cyclizations of 2-alkenyl-1,3-dicarbonyl scaffolds have been nonexistent in the literature. Driven by those facts, DFT studies were carried out using **7** as the model substrate (Scheme 8A). As shown above, substitution of one acetonitrile in Pd^{II} complex leads to an anionic intermediate **7c** (*anionic path*), with a significant reduction in free energy (**7c**, ΔG = −5.8 kcal/mol). Another possibility, like direct complexation of **7** with $Pd(CH_3CN)_2Cl_2$ (*neutral path*) after an acetonitrile substitution event, provides intermediate **7k-4** with an energy preference slightly lower than the previous one (**7k-4**, ΔG = −2.7 kcal/mol). Direct enolization of **7** (*enolate path*) resulted in a higher energy intermediate (**7′′**, ΔG = 10.8 kcal/mol), and its formation should be mediated by the palladium complex and the base. A detailed description of other reactional intermediates is described in the Supporting Information. Following the anionic pathway, π-complexation possibilities between complex **7c** and the olefin portion of the model substrate **7** were calculated, together with several ligand substitution events between acetonitrile and acetate. Free energy values showed that monosubstitution of acetonitrile ligand by one acetate, followed by π-complexation with the olefin portion to generate intermediate **7d** was the most favorable event (ΔG = −11.6 kcal/mol) (Scheme 8B). These complexes present η^2-type complexation with palladium center, with bond lengths of order of 2.2 Å (see the Supporting Information).

Next, one of the plausible pathways was considered and calculated, in which the acetate ligand deprotonates the β-ketoester carbon, resulting in enolization, showing a transition state with the highest value of free energy (**TS-1**, $\Delta\Delta G$ = 26.4 kcal/mol) among the lower anionic energy paths, which corroborates with the k_H/k_D value found in the KIE experiments. This endergonic step involves the formation of the unstable enolate intermediate **7e** (ΔG = 7.1 kcal/mol).

Scheme 7. KIE Experiments

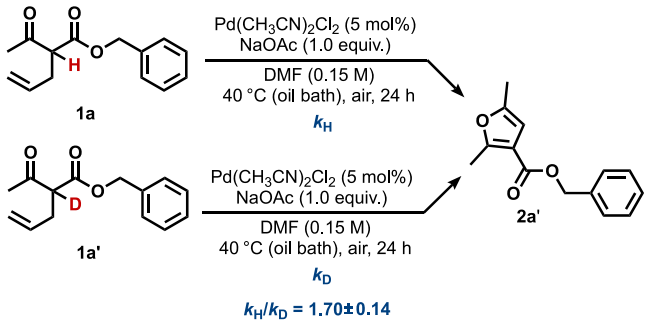

https://dx.doi.org/10.1021/acs.joc.0c02777
J. Org. Chem. 2021, 86, 3923−3942

Scheme 8. Possible Reaction Pathways and Initial Ligand Exchanges Involving Pre-complex $PdCl_2(MeCN)_2$[a]

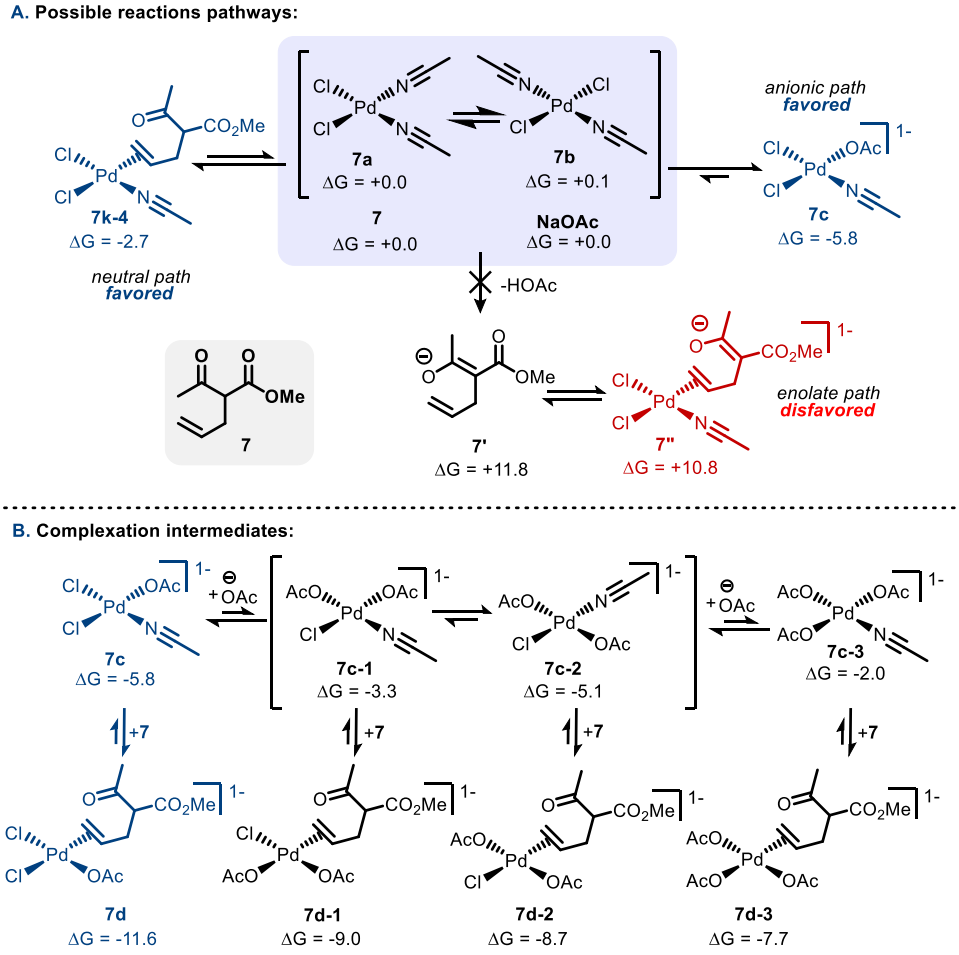

[a]Gibbs free energies in kcal/mol at M06/6-111+g(d,p)-(def2tzvp for Pd) IEF-PCM-[DMF].

The further step comprises a 5-*exo-trig* cyclization,[41] and the energies of the two possible attacks of the oxygen atom were measured (*syn* and *anti*), in which the *anti*-attack was strongly disfavored in terms of free energy barrier (**TS-3**, $\Delta\Delta G$ = 10.2 kcal/mol). A more favorable path, involving an inner-sphere *syn* insertion, was revealed to be less energetic, being initiated by the departing of AcOH by the oxygen enolate attack through an associative interchange mechanism (**TS-2**, $\Delta\Delta G$ = 5.2 kcal/mol), forming the thermodynamically favorable intermediate **7f** (ΔG = −1.2 kcal/mol). The inner-sphere *syn* insertion generates the highly strained planar square complex **7g** through **TS-4** ($\Delta\Delta G$ = 9.9 kcal/mol). In fact, Kočovskỳ and Bäckvall reported that *syn*-additions are common in the case of intramolecular oxy- and amido-palladation, when initial coordination of the internal nucleophile to the metal is observed.[42] From **7g**, all subsequent steps presented a lower energy barrier and are thermodynamically favorable. At first, **7g** undergoes into a four membered cyclic transition state **TS-5** ($\Delta\Delta G$ = 4.3 kcal/mol) to result in less strained intermediate **7h**, bearing a η^1-type complexation (bond length of 2.2 Å), with an exocyclic double bond. This bond length characterizes a weaker bond, a feature that facilitates the conversion of **7h** into a conformer that enables a β-hydride insertion event. This event is processed via another four membered transition state (**TS-6**, $\Delta\Delta G$ = 1.6 kcal/mol) to generate intermediate **7i**, presenting an agnostic interaction with the recently inserted hydrogen and the palladium core, with a bond length of 1.91 Å and Pd−H−C angle of 97°. Transition state **TS-7** characterizes a β-hydride elimination ($\Delta\Delta G$ = 2.1 kcal/mol), leading to π-complex **7j**, that suffers ligand exchange to afford product **8** and regenerate catalyst (Scheme 9).

We also evaluated a mixed neutral/anionic pathway, in which the olefin coordinates to the palladium catalyst **7a** and replace an acetonitrile ligand. Both *cis* (**7k-4**) and *trans* (**7k-2**) intermediates were explored, and the lowest energy pathway can be seen in Scheme 10 (see Scheme S2 for the pathway involving **7k-4**). Initially, we evaluated the *syn* and *anti*-attack starting from the **7k-2** intermediate, in which the reaction could proceed (see Schemes S1 for additional diastereomeric transition states). The lower energy transition state **TS-7d** involves a carbonyl attack opposed to the palladium metal, showing an energy barrier of $\Delta\Delta G$ = 14.3 kcal/mol, forming a high energy oxonium intermediate **9b** (ΔG = 11.2 kcal/mol). This intermediate could undergo barrierless steps (see Figure S172), involving the extrusion of acetonitrile and complexation of acetate ion, producing the anionic intermediate **13** (ΔG = 9.3 kcal/mol), that precedes the deprotonation of the β-ketoester carbon. A competitive pathway for these steps would involve the direct cyclization of intermediate **7d**, previously discussed without prior deprotonation, but stationary points and transition states could not be located. In subsequent steps, a low energy transition state **TS-10** ($\Delta\Delta G$ = 3.3 kcal/mol)

https://dx.doi.org/10.1021/acs.joc.0c02777
J. Org. Chem. 2021, 86, 3923−3942

Scheme 9. Relative Gibbs Energy Profile for the Anionic Path[a]

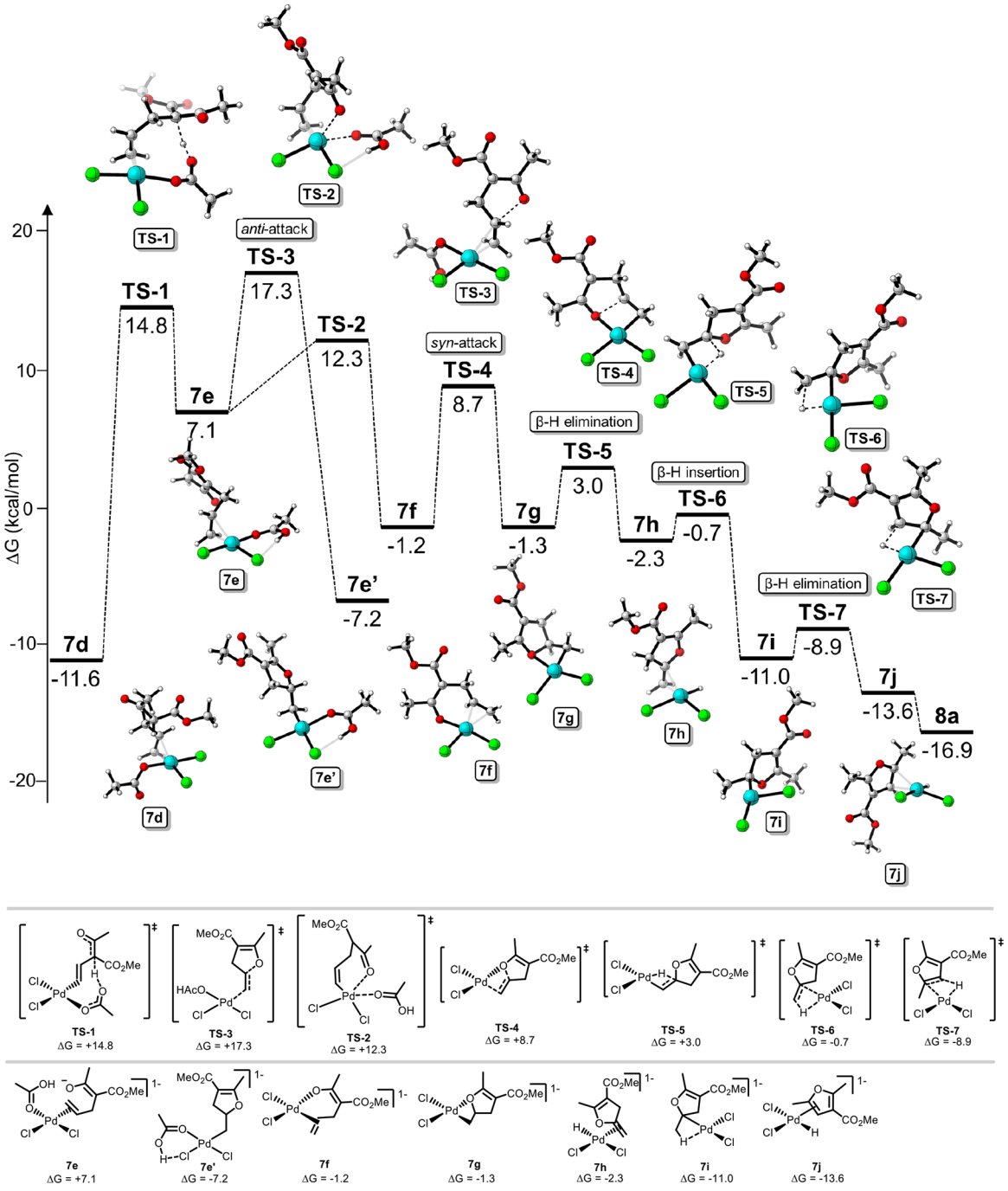

[a]Gibbs free energies in kcal/mol at M06/6-111+g(d,p)-(def2tzvp for Pd) IEF-PCM-[DMF].

characterizes deprotonation of the β-ketoester carbon by the coordinated acetate ion, leading to a dramatic decrease in energy, producing the thermodynamically favorable intermediate **14** (ΔG = −10.4 kcal/mol). All subsequent steps are related to ligand exchange events to form the reactive *cis*-complex **7g**, responsible for the first β-H elimination step and converging to the anionic mechanism previously discussed.

Analyzing the full energy profile connecting both anionic and neutral pathways, and applying the kinetic model of Kozuch and Shaik,[43] we identified the rate-limiting states **7d** and **TS-1** (anionic)/ **TS-10** (neutral), defining the energy span (δE) and kinetic of this reaction (Scheme 11). For both pathways the energy profile corroborates the conclusions obtained from the KIE experiments, suggesting the deprotonation of the β-ketoester carbon as the turnover determining states. The experimental KIE value was 1.7, whereas the calculated KIE from **TS-1** and **TS-10** geometries were 3.3 and 3.9, respectively. The lower value of the experimental KIE indicates that some elementary step must have some degree of rate control in the catalytic cycle.[44] In our scenario, the theoretical neutral pathway showed elementary steps in the catalytic cycle presenting TSs of similar energies as the C−H activation **TS-1** (Scheme 11). Considering essentially the free

https://dx.doi.org/10.1021/acs.joc.0c02777
J. Org. Chem. 2021, 86, 3923−3942

Scheme 10. Relative Gibbs Energy Profile for Mixed Neutral/Anionic Path[a]

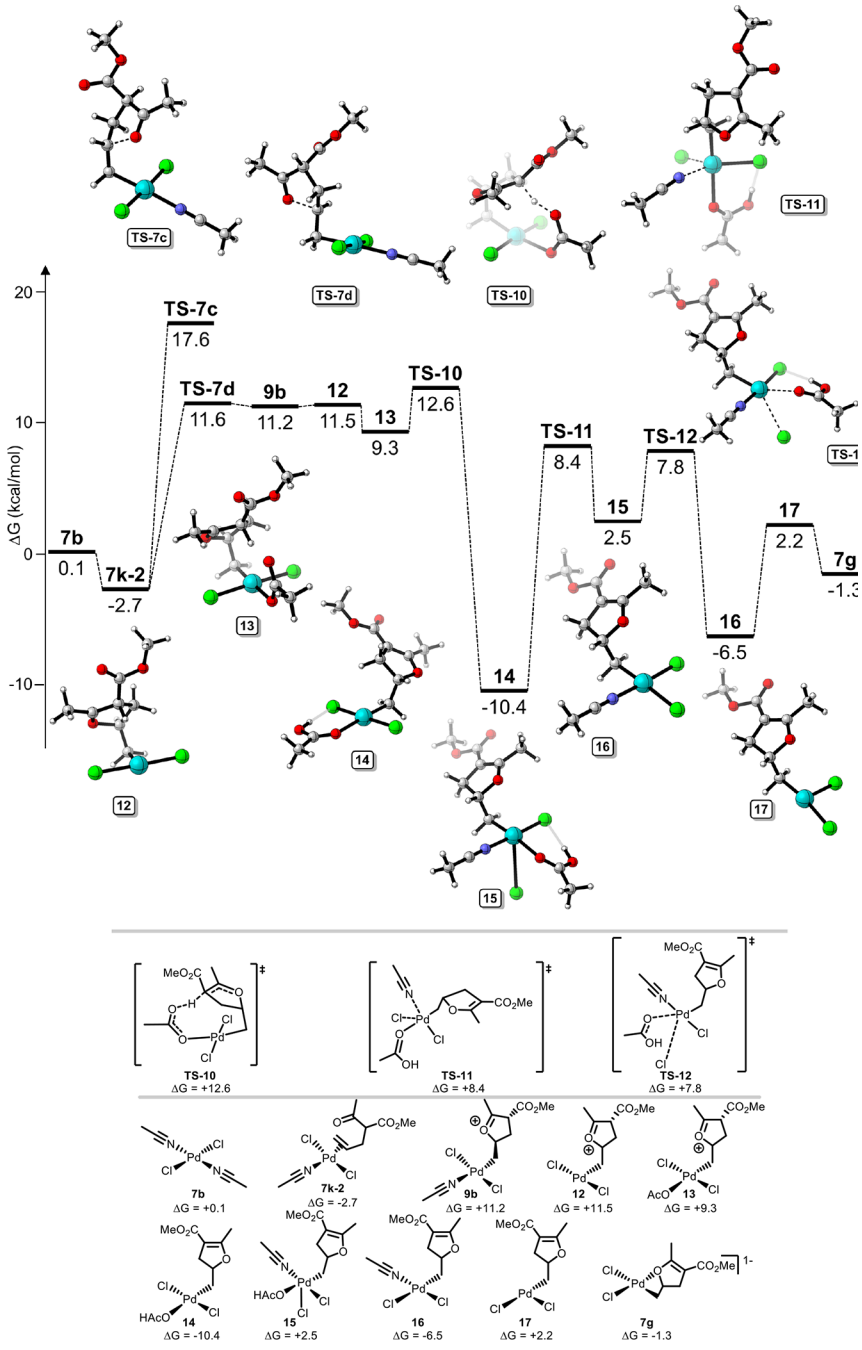

[a]Gibbs free energies in kcal/mol at M06/6-111+g(d,p)-(def2tzvp for Pd) IEF-PCM-[DMF].

energies of all the species and energy span (δE), the conclusion would be that the mixed neutral/anionic path dominates.

Parametrization and Multivariate Regression Analysis. From the previously theoretical calculations indicating the deprotonation of the β-ketoester carbon as the rate-limiting transition state, a better performance involving the electron-deficient starting materials was expected. However, a possible dichotomy between acidity and oxygen nucleophilicity in the nucleopalladation step persists. Lower yields were observed for strong electron-withdrawing groups, both in the ester and ketone portions, although no ketoester starting material remaining at the end of the reaction. In addition, the steric influence seems to have greater importance in the ketonic portion of the ketoester. Considering the lack of an obvious relationship between reactivity and structural features of the ketoesters, we decide to apply statistical correlations tools to interrogate the origin of the reaction efficiency and its relationship with the reaction mechanism.[45] Our general workflow to this study started choosing the product to collect their molecular descriptors, including calculated electronic and steric parameters (Figure 2). Initially, a conformational search of products was initiated using Molecular Mechanics (MM), followed by DFT geometry optimization (see the Supporting Information for further details). All used parameters in the models are values of the Boltzmann averaged conformers. The electronic feature of each 3-carbonyl-trisubstituted furan was

https://dx.doi.org/10.1021/acs.joc.0c02777
J. Org. Chem. 2021, 86, 3923−3942

Scheme 11. Free Energy Network Connecting Rate-Limiting States of Anionic and Neutral Pathways[a]

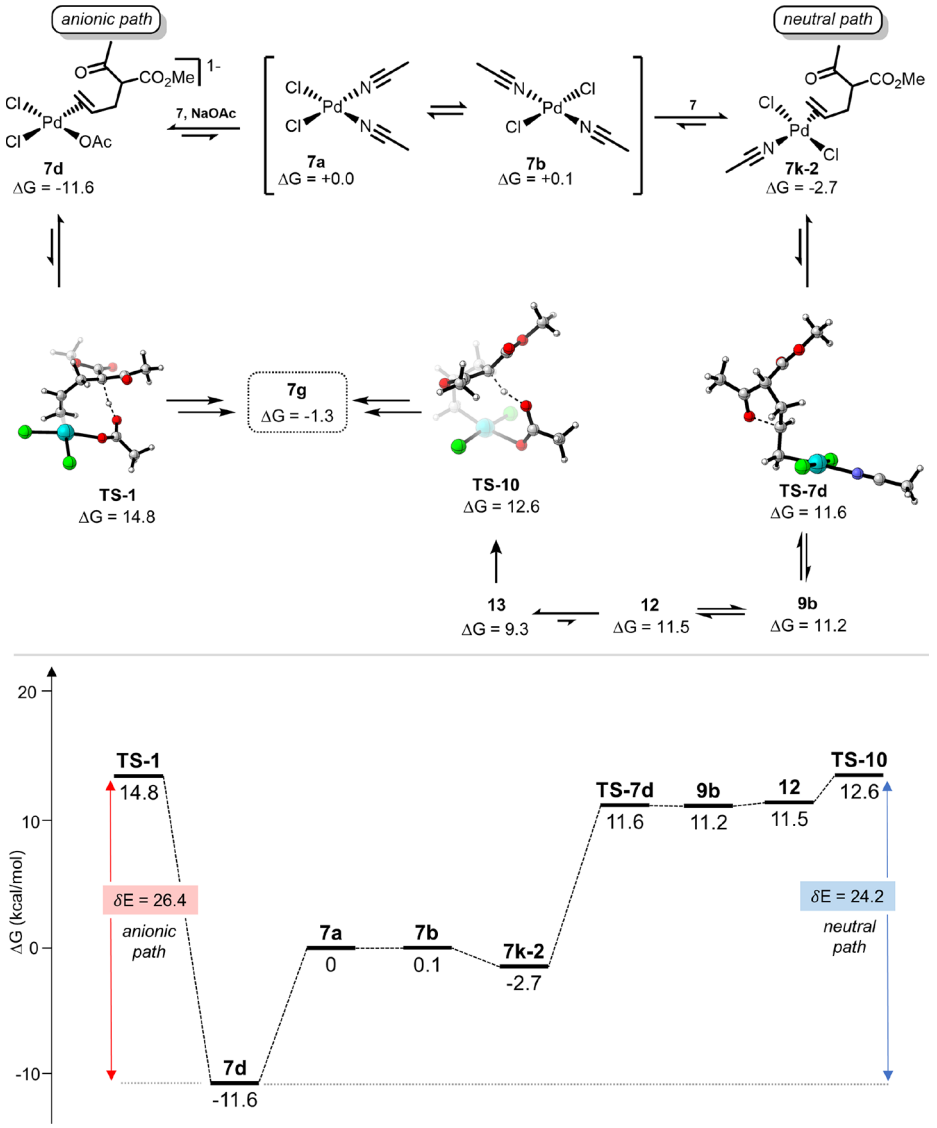

[a]Gibbs free energies in kcal/mol at M06/6-111+g(d,p)-(def2tzvp for Pd) IEFPCM-[DMF].

measured relative to the natural bond orbital (NBO) charges of oxygens (q_O) and carbons (q_C), NBO energies of lone pairs of oxygens ($E_{LP(O)}$), and $\delta_{C=O}$ and $\delta^*_{C=O}$ of the ester carbonyl fragment.[45,46] The steric effects caused by the groups attached in the carbonyl functional group were individually assessed using Verlop's Sterimol parameters L, B_1, and B_5.[47]

Next, multivariate regression analysis was carried out to investigate the cooperative impact of the electronic and steric parameters in the reaction yield, using the training set (12 samples, including R and R′ variations). The model produced good internal-validation scores (leave-one-out Q^2), k-fold, and a coefficient of determination (R^2) of 0.95 (Figure 3A). Additionally, this model described reasonably well the test set (five samples). The model overestimates the yield for the outlier **2j**, which we attributed to the underestimation of the size of isoborneol by $B_{1(R')}$ descriptor. The multivariate model was expressed in three interpretable terms, discriminating different aspects of the reaction mechanism (Figure 3A,B). The partitioning of the yield, according to these terms, helped the rationalization of their importance according to the structural features of products, as can be seen in Figure 3C.

The average energy of the π-symmetry lone pair E_{LP2_O6} describes the electron density of the ester group and is related to the decomposition of product/starting material. We assumed this hypothesis after the identification of benzylic alcohol by GC−MS during reaction monitoring analysis. The decrease in yield of products **2c**, **2d**, **2e**, and **4b** followed the increase of the electron-withdrawing group in the aromatic portion, with the descriptor E_{LP2_O6} being largely responsible for this reduction. As illustrated in Figure 3C, this term has a positive contribution for electron-rich esters **2b**,**g**−**i**,**k**, reflecting the increase in stability.

In contrast, the second hybrid stereoelectronic descriptor q_{O1}:$B_{1(R)}$ reflects the electronic and steric nature of the R group, suggesting a direct correlation with the **TS-10**, and consequently the β-hydrogen abstraction event. Electron-rich R groups make this step difficult, featuring negative values for this descriptor, such as **4f** and **4g**. In contrast, while electron-withdrawing R groups increase the yield by this descriptor,

https://dx.doi.org/10.1021/acs.joc.0c02777
J. Org. Chem. 2021, 86, 3923−3942

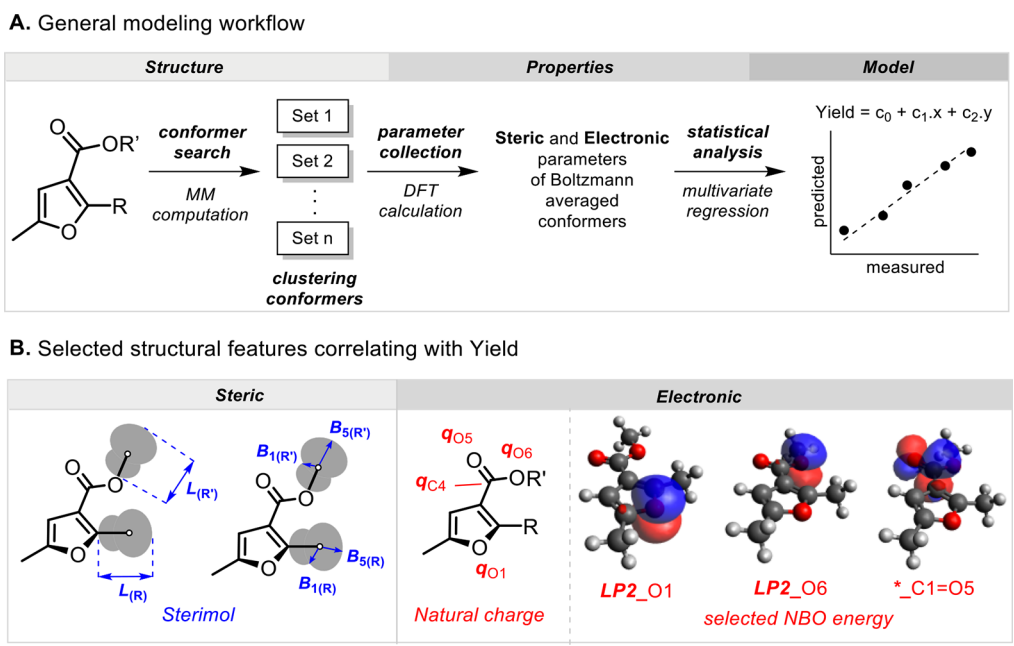

Figure 2. General modeling workflow (A) and structural features correlating with yield (B).

electron-poor R/R′ groups reinforce the drop in yield due to ester decomposition (E_{LP2_O6}), as pictured for **4b** (Figure 3C).

The third descriptor $B_{1(R)}$:$B_{1(R')}$ intercorrelates the sterics between R/R′ substituents and suggests a decreased yield in the presence of bulky groups, with higher sensitivity for R portion. Despite the highest coefficient, and therefore the greatest significance to the model, its values show little variation over the series of compounds, except for the **2h** and **4g**, containing very bulky substituents (Figure 3C). Considering that **TS-7d** and **TS-10** are close in energy, this scenario may be related to a change in the steric regime and, consequently, the rate-limiting transition state. Analyzing the geometries of these transition states, only the **TS-10** would have a greater sensitivity to the inclusion of bulky groups, especially in the R position, leading to a drastic decrease of yield and justifying the previous observations.

General Overview of Proposed Reaction Pathways. Finally, a mechanistic proposal could be illustrated to provide a general overview of the two main reaction pathways (anionic and neutral). The anionic cycle begins with ligand exchange followed by π-complexation to generate **7d**, which undergoes α-hydrogen abstraction, resulting in intermediate **7e**. Then the oxygen atom binds to the Pd core via *cis*-nucleopalladation (intermediate **7f**), and a *syn* attack in the endocyclic olefin carbon leads to **7g**. The final steps involve a β-hydride elimination to give **7h**, followed by a β-H insertion and another β-hydride elimination event (intermediates **7h** and **7i**). After proton abstraction, an acetonitrile ligand coordinates to palladium, resulting in product **8a**, that after oxidation of Pd(0) by O_2 regenerates the catalyst **7c** (Scheme 12). In the neutral path, **7b** undergoes π-complexation to generate **7k-2** and after carbonyl attack generates oxonium intermediate **9b**. After ligand exchange events, anionic intermediate **13** is produced, and deprotonation of the β-ketoester carbon by the coordinated acetate ion generates **14**. After coordination of a Cl^- (intermediate **15**) and ligand exchange, intermediate **17** leads to **7g**, and the cycle continue via the previous anionic pathway (Scheme 12).

CONCLUSIONS

In summary, we developed a mild, efficient, and greener reaction for the synthesis of 3-carbonyl-trisubstituted furan scaffolds via Pd-catalyzed Wacker-type cycloisomerization using O_2 as the sole oxidant for the process, constituting a reliable methodology for the preparation of important building blocks starting from 2-alkenyl-1,3-dicarbonyl moieties. Furthermore, experimental and computational studies made possible a detailed and unprecedented description of the reaction mechanism. This work represents a successful example of a highly detailed mechanistically aerobic cycloisomerization strategy to prepare furan-based building blocks and open new avenues toward the chemistry of potential bioactive structures.

EXPERIMENTAL SECTION

General Methods. Reagents, when not synthesized, as well as solvents were obtained commercially and when necessary were treated using standard laboratory techniques according to methods published by Perrin, Armarego, and Perrin (Pergamon Press, 1966).[48] Thin-layer chromatography analyses (TLC) using fluorescent-treated silica gel 60 (F_{254}) coated aluminum plates and revealed under UV light and/or vanillin were performed to follow up the reactions. Column chromatography using silica gel 60 (230−240 mesh) was the technique of choice for purifications. The ^1H and ^{13}C NMR spectra were recorded using the Bruker Advance 400 brand spectrometer at 400 and 100 MHz, respectively, employing $CDCl_3$ or DMSO-d_6 as solvent, using tetramethylsilane (TMS) for the ^1H NMR spectra as a reference and for the ^{13}C spectra the solvent signal was used, with the chemical displacements (δ) reported in ppm and the coupling constants (J) in hertz (Hz). The following abbreviations were used to note signal multiplicities: s, singlet; sl, singlet large; d, doublet; t, triplet; q, quartet; dd, doublet of doublets; ddd, doublet of doublet of doublets; dt, doublet of triplets; ddt, doublet of doublet of triplets; dq, doublet of quartets; m, multiplet; p, pentet; sept, septet; td, triplet of doublets; tt, triplet of triplets. The Shimadzu IR Prestige-21 spectrophotometer was used to obtain infrared spectra with wavelength absorbances (cm^{-1}). Melting point analyses were performed on a melting point M-560 (BUCHI) apparatus, and high-resolution mass spectra were recorded using a Bruker model IMPACT HD spectrometer operating in positive mode and electrospray ionization source with quadrupole time-of-flight analyzer

https://dx.doi.org/10.1021/acs.joc.0c02777
J. Org. Chem. 2021, 86, 3923−3942

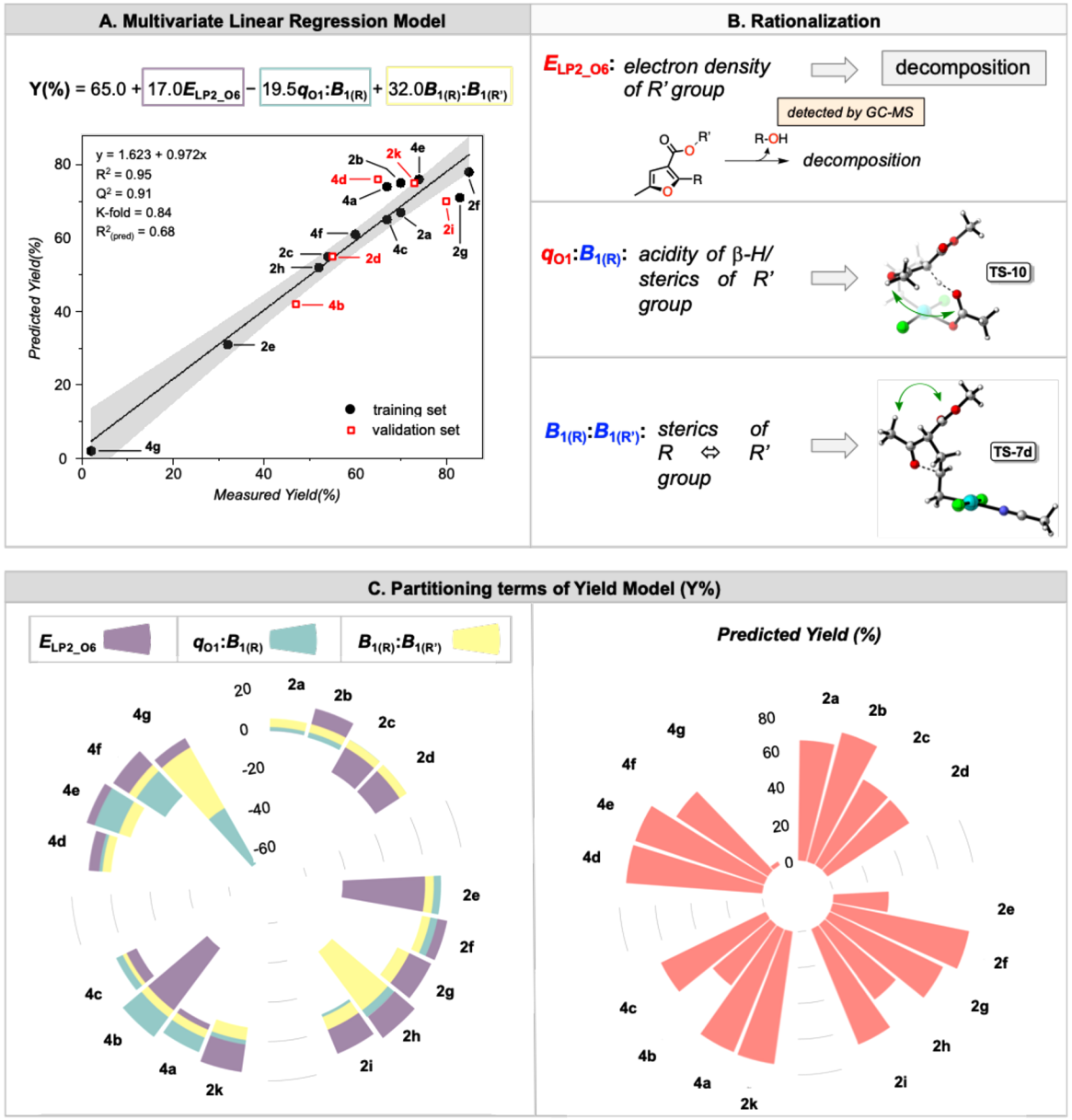

Figure 3. Mechanistic investigation by multidimensional regression modeling. (A) and (B) E_{LP2_O6}, descriptor of average energy of the π-symmetry lone pair; q_{O1}:$B_{1(R)}$, second hybrid stereoelectronic descriptor; $B_{1(R)}$:$B_{1(R')}$, descriptor that intercorrelates the sterics between R/R′ substituents. (C) The partitioning of the yield with positive and negative contributions of descriptors presented in model Y (%) = 65.0 + E_{LP2_O6} − q_{O1}:$B_{1(R)}$ + $B_{1(R)}$:$B_{1(R')}$.

(ESI-QqTOF). Optical rotations were measured on a PerkinElmer Polarimeter. ***Warning:*** *despite the absence of any accidents involving the use of oxygen gas in the adopted synthetic procedures, all experiments were conducted in a controlled environment, composed of a fume hood with appropriate exhaust. All experiments were conducted without pressurization.*

Preparation of 2-Alkenyl-β-ketoester Derivatives. Method I. The following procedure was adapted from literature.[49] The β-ketoester (10.4 mmol, 1.00 equiv), acetone (30 mL), and potassium carbonate (13.5 mmol, 1.30 equiv) were added in an ace tube, respectively. Allyl bromide (13.5 mmol, 1.30 equiv) was added, and the mixture was stirred overnight at 60 °C using a an oil bath. After completion, the reaction was filtered, and the solvent was evaporated under reduced pressure. The crude product was purified by flash silica column chromatography using a mixture of hexane and ethyl acetate (9:1) as eluent.

Protocol for Transesterification Reactions. Method II. The following procedure was adapted from the literature. Methyl 2-acetylpent-4-enoate (7) (20 mmol, 1.0 equiv), the respective alcohol (30 mmol, 1.5 equiv), and catalyst (2 mmol, 0.1 equiv, boric acid,[50] or iron nanoparticle[51]), were added in a round-bottom flask with toluene (100 mL). The mixture was refluxed using a an oil bath under vigorous stirring for 12 h using a Dean−Stark apparatus. After completion, the solvent was evaporated under reduced pressure, and the crude product was purified by flash silica column chromatography using a mixture of hexane and ethyl acetate (9:1) as eluent.

Preparation of Substituted Dicarbonyl-2-alkenyl Derivatives. Method III. The following procedure was adapted from the literature.[21,52,53] In a 100 mL round-bottom flask charged with distilled water (3.0 mL) were slowly added NaOH (0.60 g, 15 mmol, 0.75 equiv) and ethanol (50 mL), a mixture of benzaldehyde (2.1 mL, 20 mmol, 1.0 equiv), and acetophenone (2.4 mL, 20 mmol, 1.0 equiv) with the temperature being maintained by an ice bath. The reaction mixture was stirred and allowed to reach room temperature for 4 h. After the end of the reaction, the product (chalcone) has precipitated, and it was filtered and washed it with water and ice-cold ethanol. The

https://dx.doi.org/10.1021/acs.joc.0c02777
J. Org. Chem. 2021, 86, 3923−3942

Scheme 12. Mechanistic Proposal

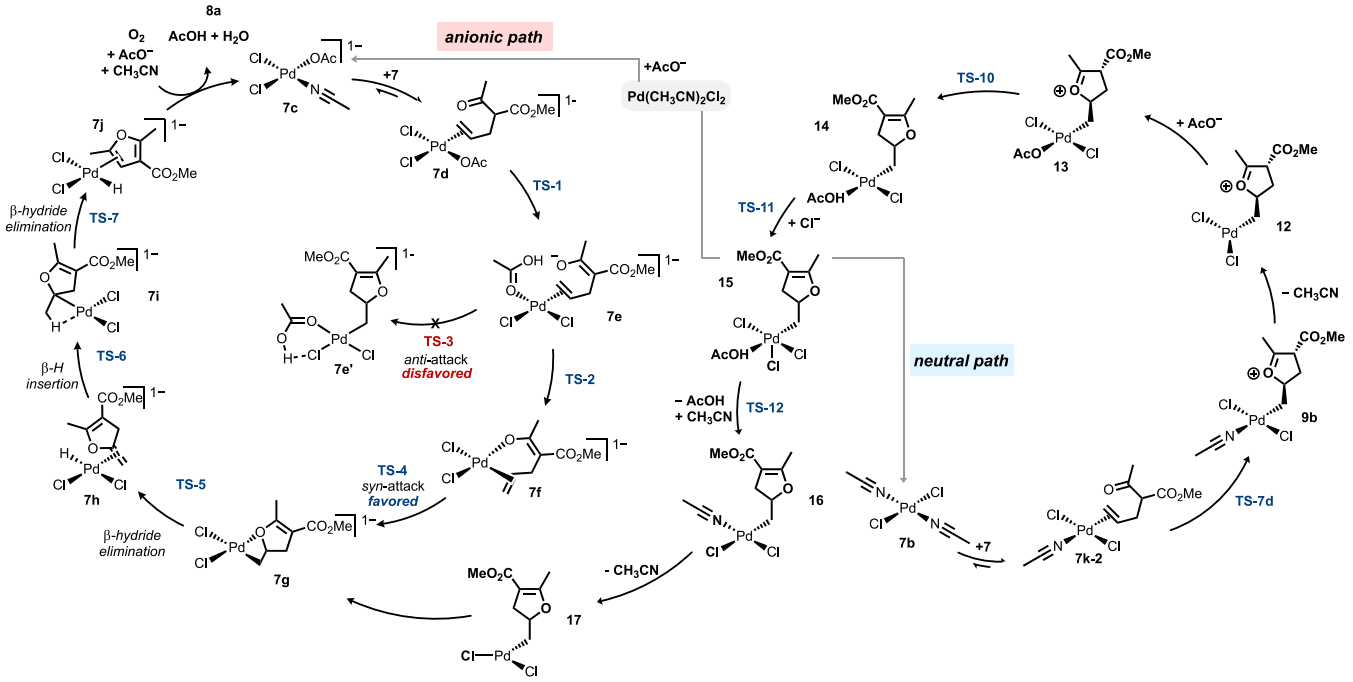

resulting chalcone was used without further purification. Next, chalcone (0.30 g, 1.5 mmol, 1.0 equiv) was solubilized in ethanol (5 mL), and the mixture was cooled to 0 °C. A solution of $NaBH_4$ (0.12 g, 3.0 mmol, 2.0 equiv) in water (1 mL) was and slowly added. The reaction was stirred in an ice bath for 1 h and then for another 2 h at room temperature. The reaction was extracted with the addition of 10 mL of distilled water and ether (5 × 10 mL), and the organic phase was dried with anhydrous Na_2SO_4. The resulting alcohol was used without further purification. In a 15 mL round-bottom flask charged with alcohol (0.11 g, 0.50 mmol, 1.0 equiv) were added 1,3-dicarbonyl (0.60 mmol, 1.2 equiv) and DCM (2 mL), Re_2O_7 catalyst (0.0036 g, 0.0075 mmol, 0.015 equiv), and the reaction was stirred at room temperature. The complete consumption of the starting materials was monitored by TLC, and NH_4Cl solution (1.0 mL) was added. The mixture was extracted with EtOAc (3 × 10 mL) and the organic phase dried with anhydrous Na_2SO_4. The solvent was removed, and the crude product was purified by column chromatography using silica gel and a hexane/EtOAc gradient.

Pd-Catalyzed Aerobic Cycloisomerization Reactions. Method IV. In a dry 5 mL round-bottom flask, the previously prepared 2-alkenyl-β-ketoesters (0.3 mmol, 1.0 equiv), preactivated 4 Å molecular sieves powder (80 mg), dry sodium acetate (0.3 mmol, 1.0 equiv), $PdCl_2(CH_3CN)_2$ (5 mol %, 0.0075 mmol), and DMF (2.0 mL) were added in sequence. An O_2 atmosphere was achieved, and the reaction was stirred at 40 °C using a an oil bath for 24 h. After completion, the crude product was purified by flash silica column chromatography using a mixture of hexane/ethyl acetate (9:1) as eluent.

*Preparation of Deuterated Compound **1a**′. Method V.* The following procedure was adapted from the literature.[54] The β-ketoester **1a** (0.23 g, 1.00 mmol) was weighed in a 5 mL round-bottom flask in which was added a volume of 1.0 mL of a 50 mg/mL (0.40 mol/L) K_2CO_3 solution prepared in D_2O. The resulting solution was stirred at room temperature for 24 h. The crude product was extracted with diethyl ether (3 × 5 mL), and the organic phase was dried with anhydrous Na_2SO_4. The product (2-D-benzyl 2-acetylpent-4-enoate (**1a**′)) was obtained after simple filtration and solvent removal.

NMR Experiments. Substrate **1a** (0.020 mmol, 0.0046 g), NaOAc (0.020 mmol, 0.0016 g), and $PdCl_2(CH_3CN)_2$ (0.020 mmol, 0.0052 g), were weighed separately in 1.5 mL microtubes (Eppendorf, Safe-Lock). Deuterated DMF (0.7 mL) was added to the tube containing **1a**, the mixture was sonicated in an ultrasound bath and transferred to an NMR tube, and a ^1H NMR spectrum was recorded. In sequence, the reaction solution was transferred to the tube containing the NaOAc base, sonicated, and transferred to the same NMR tube, in which a second ^1H NMR spectrum was recorded. Finally, the final solution was transferred to the tube containing the Pd catalyst, sonicated, and transferred to the same NMR tube, and a final ^1H NMR spectrum was recorded. Each spectrum was recorded with an interval of 32 and 24 min between them.

Kinetics. In a 10 mL round-bottom flask were added compound **1a** (105 mg, 0.50 mmol, 1.00 equiv) or deuterated compound **1a**′ (71 mg, 0.40 mmol, 1.00 equiv), dry NaOAc (1.00 equiv), $Pd(CH_3CN)_2Cl_2$ (5 mol %), and the internal standard hexadecane (0.50 equiv). Then DMF was added to complete a 0.15 M solution of the respective β-ketoester (**1a** or **1a**′), and the reaction flask was kept open under stirring at 40 °C using a an oil bath for 24 h. At every 30 s for the first 3 min of reaction and then for every 5 min (see the Supporting Information), a 70 μL aliquot of the reaction was collected using a micropipette, which was diluted with HPLC grade ethyl acetate in a sufficient amount to complete 1000 μL of solution. Three runs were performed on the CG−MS equipment, each with an injection volume of 1 μL of the resulting solution, and the relative number of analytes were obtained. Details of the procedure for performing GC analysis were described in the Supporting Information.

Computational Methods. All DTF calculations were performed using the ultrafine grid in Gaussian 16.[55] Geometry optimization and single-point calculations of intermediates and transition states were conducted with M06 functional[56] using mixed basis-set of def2TZVP[57] for palladium e 6-311+g(d,p)[58] for other atoms. Vibrational analysis was performed at all calculated points to confirm they either as a transition state (only one imaginary frequency) or as a local minimum (zero imaginary frequencies), furnishing also the zero-point vibrational energies, the thermal and entropic correction from which the Gibbs free energies were determined. Solvent effects were accounted for all optimizations using IEF-PCM (*N*,*N*-dimethylformamide). Transition states were submitted to intrinsic reaction coordinate (IRC) calculation to confirm the desired connection between reactants and products. Where relevant, conformational search of intermediates was performed using SPMC (Systematic

https://dx.doi.org/10.1021/acs.joc.0c02777
J. Org. Chem. 2021, 86, 3923−3942

Pseudo Monte Carlo) with OPLS_2005 force field as implemented in Maestro 9.6 software.[59] Visualizations were done using GaussView 5[60] and CYLView 2.0.[61] See the Supprting Information for detailed information on the parametrization process.

*Benzyl 2-Acetylpent-4-enoate (**1a**).*[62] Synthesized according to method I, furnishing the known compound in 48% (4.9 mmol, 1.2 g) isolated yield as a pale-yellow oil, R_f 0.27 (10% ethyl acetate in hexane). ^{1}H NMR (400 MHz, $CDCl_3$): δ 7.39−7.30 (m, 5H), 5.73 (ddt, J = 17.0, 10.2, 6.8 Hz, 1H), 5.16 (d, J = 1.2 Hz, 2H), 5.07 (dq, J = 17.1, 1.5 Hz, 1H), 5.03 (dq, J = 10.2, 1.3 Hz, 1H), 3.57 (t, J = 7.4 Hz, 1H), 2.63−2.58 (m, 2H), 2.18 (s, 3H). ^{13}C{^{1}H} NMR (100 MHz, $CDCl_3$): δ 202.3, 169.1, 135.3, 134.1, 128.7, 128.6, 128.4, 117.6, 67.2, 59.2, 32.2, 29.2. IR (NaCl, thin film, cm^{-1}): 3218, 3185, 3131, 3108, 3073, 1893, 1866, 1793, 1650, 1606, 1509, 1415, 1378, 1335, 1301, 1145, 1071, 901, 849.

*4-Methoxybenzyl 2-acetylpent-4-enoate (**1b**).* Synthesized according to method II, furnishing the new compound in 72% (3.6 mmol, 0.93 g) isolated yield as a yellow oil, R_f 0.44 (20% ethyl acetate in hexane). ^{1}H NMR (400 MHz, $CDCl_3$): δ 7.33−7.22 (m, 2H), 6.92−6.83 (m, 2H), 5.72 (ddt, J = 17.0, 10.2, 6.8 Hz, 1H), 5.10 (d, J = 2.3 Hz, 2H), 5.09−5.00 (m, 2H), 3.80 (s, 3H), 3.54 (t, J = 7.4 Hz, 1H), 2.61−2.56 (m, 2H), 2.16 (s, 3H). ^{13}C{^{1}H} NMR (100 MHz, $CDCl_3$): δ 202.4, 169.2, 159.9, 134.2, 130.4, 127.5, 117.6, 114.1, 67.1, 59.3, 55.4, 32.2, 29.2. IR (NaCl, thin film, cm^{-1}): 3078, 3003, 2959, 2938, 2837, 1742, 1715, 1643, 1614, 1587, 1516, 1464, 1443, 1360, 1304, 1250, 1175, 1150, 1113, 1034, 922, 827. HRMS (ESI-TOF) m/z: [M + Na]$^+$ Calcd for $C_{15}H_{18}O_4Na$ 285.1098; Found, 285.1087.

*Methyl 4-(((2-Acetylpent-4-enoyl)oxy)methyl)benzoate (**1c**).* Synthesized according to method II, furnishing the new compound in 23% (0.8 mmol, 0.2 g) isolated yield as a pale-yellow oil, R_f 0.24 (10% ethyl acetate in hexane). ^{1}H NMR (400 MHz, $CDCl_3$): δ 8.05−8.00 (m, 2H), 7.44−7.37 (m, 2H), 5.73 (ddt, J = 17.0, 10.2, 6.8 Hz, 1H), 5.21 (d, J = 0.9 Hz, 2H), 5.12−5.01 (m, 2H), 3.91 (s, 3H), 3.59 (t, J = 7.4 Hz, 1H), 2.63−2.58 (m, 2H), 2.19 (s, 3H). ^{13}C{^{1}H} NMR (100 MHz, $CDCl_3$): δ 202.2, 169.0, 166.7, 140.3, 134.0, 130.3, 130.0, 128.0, 117.8, 66.4, 59.2, 52.3, 32.3, 29.3. IR (KBr, thin film, cm^{-1}): 3078, 3003, 2981, 2953, 2843, 1745, 1728, 1714, 1643, 1614, 1577, 1512, 1435, 1417, 1359, 1311, 1282, 1226, 1180, 1149, 1111, 1056, 1020, 993, 966, 921, 854, 802, 758, 704. HRMS (ESI-TOF) m/z: [M + H]$^+$ Calcd for $C_{16}H_{19}O_5$ 291.1227; Found, 291.1217.

*4-Chlorobenzyl 2-Acetylpent-4-enoate (**1d**).* Synthesized according to method II, furnishing the new compound in 20% (0.4 mmol, 0.2 g) isolated yield as a yellow oil, R_f0.57 (20% ethyl acetate in hexane). ^{1}H NMR (400 MHz, $CDCl_3$): δ 7.35−7.31 (m, 2H), 7.29−7.25 (m, 2H), 5.72 (ddt, J = 17.0, 10.2, 6.8 Hz, 1H), 5.14−5.11 (m, 2H), 5.09−5.00 (m, 2H), 3.57 (t, J = 7.4 Hz, 1H), 2.63−2.57 (m, 2H), 2.19 (s, 3H). ^{13}C{^{1}H} NMR (100 MHz, $CDCl_3$): δ 202.2, 169.0, 134.4, 134.0, 133.9, 129.8, 128.9, 117.7, 66.3, 59.2, 32.2, 29.3. IR (NaCl, thin film, cm^{-1}): 3080, 3003, 2982, 2957, 2924, 1746, 1715, 1643, 1601, 1495, 1435, 1360, 1227, 1184, 1150, 1094, 1016, 993, 922, 806. HRMS (ESI-TOF) m/z: [M + H]$^+$ Calcd for $C_{14}H_{16}ClO_3$ 267.0782; Found, 267.0773.

*4-Nitrobenzyl 2-Acetylpent-4-enoate (**1e**).* Synthesized according to method II, furnishing the new compound in 24% (0.5 mmol, 0.1 g) isolated yield as a yellow oil, R_f 0.57 (20% ethyl acetate in hexane). ^{1}H NMR (400 MHz, $CDCl_3$): δ 8.26−8.20 (m, 2H), 7.50 (m, 2H), 5.74 (ddt, J = 17.0, 10.2, 6.8 Hz, 1H), 5.27−5.24 (m, 2H), 5.12−5.04 (m, 2H), 3.63 (t, J = 7.4 Hz, 1H), 2.65−2.60 (m, 2H), 2.23 (s, 3H). ^{13}C{^{1}H} NMR (100 MHz, $CDCl_3$): δ 202.2, 169.0, 148.0, 142.6, 133.9, 128.7, 124.0, 118.0, 65.7, 59.1, 32.4, 29.5. IR (NaCl, thin film, cm^{-1}): 3113, 3082, 2982, 2951, 2859, 1746, 1715, 1643, 1607, 1520, 1435, 1348, 1265, 1227, 1182, 1150, 1113, 1057, 995, 924, 853, 739. HRMS (ESI-TOF) m/z: [M + H]$^+$ Calcd for $C_{14}H_{16}NO_5$ 278.1023; Found, 278.1015.

*Octyl 2-Acetylpent-4-enoate (**1f**).* Synthesized according to method II, furnishing the new compound in 40% (1.4 mmol, 0.36 g) isolated yield as an orange oil, R_f 0.47 (20% ethyl acetate in hexane). ^{1}H NMR (400 MHz, DMSO): δ 5.72 (ddt, J = 17.0, 10.2, 6.7 Hz, 1H), 5.08 (dq, J = 17.1, 1.6 Hz, 1H), 5.00 (dq, J = 10.2, 1.2 Hz, 1H), 4.07 (td, J = 6.6, 1.4 Hz, 2H), 3.74 (dd, J = 6.6, 6.5 Hz, 1H), 2.53−2.39 (m, 2H), 2.18−2.17 (m, 3H), 1.61−1.49 (m, 2H), 1.27 (m, 10H), 0.86 (t, J = 6.9 Hz, 3H). ^{13}C{^{1}H} NMR (100 MHz, DMSO): δ 202.6, 169.0, 134.8, 117.0, 64.7, 58.0, 39.5, 31.6, 31.2, 29.0, 28.6, 28.5, 28.0, 25.3, 22.1, 13.9. IR (NaCl, thin film, cm^{-1}): 3080, 2957, 2928, 2857, 1746, 1715, 1643, 1468, 1435, 1358, 1231, 1184, 1152, 1061, 993, 918. HRMS (ESI-TOF) m/z: [M + H]$^+$ Calcd for $C_{15}H_{27}O_3$, 255.1960; Found, 255.1959.

*Decan-2-yl 2-Acetylpent-4-enoate (**1g**).* Synthesized according to method II, furnishing the new compound in 95% (4.6 mmol, 1.4 g) isolated yield as a translucent oil, R_f0.22 (10% ethyl acetate in hexane). ^{1}H NMR (400 MHz, $CDCl_3$): δ 5.73 (m, 1H), 5.08 (dq, J = 17.1, 1.5 Hz, 1H), 5.03 (dq, J = 10.2, 1.2 Hz, 1H), 4.98−4.89 (m, 1H), 3.47 (t, J = 7.4 Hz, 1H), 2.60−2.54 (m, 2H), 2.21 (s, 3H), 1.31−1.18 (m, 17H), 0.86 (t, J = 6.9 Hz, 3H). ^{13}C{^{1}H} NMR (100 MHz, $CDCl_3$): δ 202.5, 169.0, 134.4, 117.5, 72.6, 59.6, 35.9, 32.2, 32.0, 29.7, 29.4, 29.1, 25.5, 22.8, 19.9, 14.2. IR (NaCl, thin film, cm^{-1}): 3080, 2926, 2855, 1740, 717, 1643, 1466, 1439, 1379, 1358, 1327, 1246, 1231, 1186, 1155, 1121, 1061, 995, 916. HRMS (ESI-TOF) m/z: [M + Na]$^+$ Calcd for $C_{17}H_{30}O_3Na$ 305.2088; Found, 305.2096.

*tert-Butyl 2-Acetylpent-4-enoate (**1h**).*[63] Synthesized according to method II, furnishing the known compound in 15% (0.7 mmol, 0.1 g) isolated yield as a translucent oil, R_f 0.48 (10% ethyl acetate in hexane). ^{1}H NMR (400 MHz, $CDCl_3$): δ 5.72 (ddt, J = 17.0, 10.2, 6.8 Hz, 1H), 5.07 (dq, J = 17.1, 1.6 Hz, 1H), 5.02 (dq, J = 10.2, 1.1 Hz, 1H), 3.40 (t, J = 7.4 Hz 1H), 2.53 (m, 2H), 2.21−2.20 (m, 3H), 1.44 (s, 9H). ^{13}C{^{1}H} NMR (100 MHz, $CDCl_3$): δ 202.9, 168.5, 134.6, 117.3, 82.1, 60.4, 32.3, 29.1, 28.0. IR (NaCl, thin film, cm^{-1}): 3080, 3003, 2980, 2934, 1738, 1715, 1643, 1479, 1456, 1435, 1393, 1369, 1339, 1252, 1146, 997, 918, 845.

*(1RS,2SR,5RS)-2-Isopropyl-5-methylcyclohexyl 2-Acetylpent-4-enoate (**1i**).* Synthesized according to method II, furnishing the new compound in 13% (0.34 mmol, 0.094 g) isolated yield as a pale-orange oil, R_f 0.63 (10% ethyl acetate in hexane). ^{1}H NMR (400 MHz, $CDCl_3$): δ 5.79−5.68 (m, 1H), 5.24 (m, 1H), 5.13−5.01 (m, 2H), 3.52 (td, J = 7.5, 2.0 Hz, 1H), 2.62−2.57 (m, 2H), 2.23 (d, J = 1.6 Hz, 3H), 2.01−1.89 (m, 1H), 1.79−1.70 (m, 2H), 1.60−1.47 (m, 1H), 1.33 (m, 2H), 1.11−0.90 (m, 3H), 0.86 (m, 9H). ^{13}C{^{1}H} NMR (100 MHz, $CDCl_3$): δ 202.5, 168.8, 134.4, 117.5, 72.7, 59.8, 46.9, 39.1, 34.8, 32.2, 29.2, 26.7, 25.3, 22.2, 21.2, 20.8. IR (NaCl, thin film, cm^{-1}): 3080, 2949, 2924, 2870, 2847, 1736, 1717, 1643, 1476, 1456, 1445, 1389, 1369, 1358, 1321, 1246, 1233, 1192, 1144, 1063, 1024, 1009, 993, 918. HRMS (ESI-TOF) m/z: [M + Na]$^+$ Calcd for $C_{17}H_{28}O_3Na$ 303.1931; Found, 303.1934.

*(1RS,2RS,4SR)-7,7-Dimethylbicyclo[2.2.1]heptan-2-yl 2-Acetylpent-4-enoate (**1j**).* Synthesized according to method II, furnishing the new compound in 8% (0.28 mmol, 0.080 g) isolated yield as a translucent oil, R_f 0.55 (10% ethyl acetate in hexane). ^{1}H NMR (400 MHz, $CDCl_3$): δ 5.81−5.69 (m, 1H), 5.01 (dq, J = 17.0, 1.5 Hz, 1H), 5.07−5.03 (m, 1H), 4.94−4.89 (m, 1H), 3.54 (td, J = 7.4, 1.5 Hz, 1H), 2.63−2.57 (m, 2H), 2.24 (s, 3H), 1.91−1.66 (m, 3H), 1.36−1.16 (m, 2H), 0.90−0.82 (m, 9H). ^{13}C{^{1}H} NMR (100 MHz, $CDCl_3$): δ 202.6, 169.6, 134.4, 117.6, 81.4, 59.6, 48.0, 44.9, 36.7, 32.3, 29.2, 28.1, 27.2, 19.8, 18.9, 13.6. IR (NaCl, thin film, cm^{-1}): 3078, 2955, 2880, 1740, 1717, 1643, 1481, 1454, 1439, 1391, 1358, 1304, 1248, 1233, 1188, 1155, 1115, 1047, 1018, 993, 916. HRMS (ESI-TOF) m/z: [M + Na]$^+$ Calcd for $C_{17}H_{26}O_3Na$ 301.1775; Found, 301.1762.

*(3S,8S,9S,10R,13R,14S,17R)-10,13-Dimethyl-17-((R)-6-methylheptan-2-yl)-2,3,4,7,8,9,10,11,12,13,14,15,16,17-tetradecahydro-1H-cyclopenta[a]phenanthren-3-yl 2-Acetylpent-4-enoate (**1k**).* Synthesized according to method II, furnishing the new compound in 25% (0.9 mmol, 0.4 g) isolated yield as a white solid, mp 75.8−77.7 °C, R_f 0.63 (10% ethyl acetate in hexane), $[\alpha]_D^{25}$ −16.9 (c 0.5, AcOEt). ^{1}H NMR (400 MHz, $CDCl_3$): δ 5.80−5.68 (m, 1H), 5.40−5.35 (m, 1H), 5.09 (dq, J = 17.1, 1.5 Hz, 1H), 5.06−5.02 (m, 1H), 4,71−4.72 (m, 1H), 3.48 (t, J = 7.4 Hz, 1H), 2.60−2.55 (m, 2H), 2.23 (s, 3H), 2.05−1.76 (m, 6H), 1.70−0.89 (m, 30H), 0.86 (dd, J = 6.6, 1.8 Hz, 6H), 0.67 (s, 3H). ^{13}C{^{1}H} NMR (100 MHz, $CDCl_3$): δ 202.6, 168.8, 139.4, 134.4, 123.1, 117.5, 75.3, 59.6, 56.8, 56.3, 50.1,

https://dx.doi.org/10.1021/acs.joc.0c02777
J. Org. Chem. 2021, 86, 3923−3942

42.4, 39.6, 38.0, 37.0, 36.7, 36.3, 35.9, 32.3, 32.0, 29.1, 28.4, 27.8, 24.4, 23.0, 21.2, 19.4, 18.8, 12.0. IR (KBr pellet, cm^{-1}): 2967, 2947, 2889, 2868, 2855, 1746, 1717, 1643, 1468, 1381, 1360, 1244, 1196, 1138, 1026, 995, 918. HRMS (ESI-TOF) m/z: $[M + NH_4]^+$ Calcd for $C_{34}H_{58}O_3N$ 528.4412; Found, 528.4425.

*Benzyl 2,5-Dimethylfuran-3-carboxylate (**2a**).* Synthesized according to method IV, furnishing the new compound in 70% (0.21 mmol, 0.055 g) isolated yield as a yellow oil, R_f 0.45 (10% ethyl acetate in hexane). ^1H NMR (400 MHz, $CDCl_3$): δ 7.44−7.30 (m, 5H), 6.27 (s, 1H), 5.28 (s, 2H), 2.54 (s, 3H), 2.24 (s, 3H). $^{13}C\{^1H\}$ NMR (100 MHz, $CDCl_3$): δ 164.1, 158.0, 150.1, 136.5, 128.6, 128.1, 128.1, 113.8, 106.3, 65.8, 13.8, 13.2. IR (NaCl, thin film, cm^{-1}): 3123, 3090, 3065, 3034, 2953, 2924, 2891, 2857, 1722, 1715, 1622, 1587, 1499, 1454, 1418, 1402, 1362, 1279, 1233, 1198, 1132, 1074, 1030, 988, 926, 814, 775, 752, 745, 735, 696. HRMS (ESI-TOF) m/z: $[M + H]^+$ Calcd for $C_{14}H_{15}O_3$ 231.1016; Found, 231.1006.

*4-Methoxybenzyl 2,5-Dimethylfuran-3-carboxylate(**2b**).* Synthesized according to method IV, furnishing the new compound in 70% (0.22 mmol, 0.054 g) isolated yield as a white solid, mp 38.7−39.4 °C, R_f 0.47 (10% ethyl acetate in hexane). ^1H NMR (400 MHz, $CDCl_3$): δ 7.36−7.30 (m, 2H), 6.93−6.86 (m, 2H), 6.22 (d, J = 0.8 Hz, 1H), 5.19 (s, 2H), 3.81 (s, 3H), 2.51 (s, 3H), 2.22 (d, J = 0.5 Hz, 3H). $^{13}C\{^1H\}$ NMR (100 MHz, $CDCl_3$): δ 164.3, 159.6, 158.0, 150.0, 130.0, 128.6, 114.0, 113.9, 106.3, 65.7, 55.4, 13.9, 13.3. IR (KBr pellet, cm^{-1}): 3123, 3073, 3048, 2994, 2974, 2961, 2938, 2920, 2839, 1709, 1612, 1585, 1516, 1450, 1400, 1371, 1306, 1281, 1258, 1244, 1202, 1188, 1072, 1038, 982, 922, 833, 820, 779. HRMS (ESI-TOF) m/z: $[M + Na]^+$ Calcd for $C_{15}H_{16}O_4Na$ 283.0941; Found, 283.0928.

*4-(Methoxycarbonyl)benzyl 2,5-Dimethylfuran-3-carboxylate (**2c**).* Synthesized according to method IV, furnishing the new compound in 54% (0.16 mmol, 0.047 g) isolated yield as a white solid, mp 72−74.4 °C, R_f 0.43 (10% ethyl acetate in hexane). ^1H NMR (400 MHz, $CDCl_3$): δ 8.06−8.00 (m, 2H), 7.47−7.43 (m, 2H), 6.24 (d, J = 1.0 Hz, 1H), 5.30 (s, 2H), 3.91 (s, 3H), 2.52 (s, 3H), 2.24 (sl, 3H). $^{13}C\{^1H\}$ NMR (100 MHz, $CDCl_3$): δ 166.9, 164.0, 158.4, 150.3, 141.6, 130.0, 129.9, 127.6, 113.5, 106.2, 65.1, 52.3, 13.9, 13.3. IR (KBr pellet, cm^{-1}): 2999, 2955, 2930, 1728, 1701, 1614, 1585, 1449, 1435, 1406, 1368, 1279, 1227, 1200, 1117, 1107, 1084, 1020, 995, 964, 843, 814, 773, 750. HRMS (ESI-TOF) m/z: $[M + H]^+$ Calcd for $C_{16}H_{17}O_5$289.1070; Found, 289.1062.

*4-Chlorobenzyl 2,5-Dimethylfuran-3-carboxylate (**2d**).* Synthesized according to method IV, furnishing the new compound in 55% (0.08 mmol, 0.02 g) isolated yield as a yellow oil, R_f 0.88 (20% ethyl acetate in hexane). ^1H NMR (100 MHz, $CDCl_3$): δ 7.34−7.32 (m, 4H), 6.22 (d, J = 0.8 Hz, 1H), 5.21 (s, 2H), 2.52 (s, 3H), 2.23 (d, J = 0.6 Hz, 3H). $^{13}C\{^1H\}$ NMR (100 MHz, $CDCl_3$): δ 164.1, 158.3, 150.2, 135.0, 134.2, 129.5, 128.9, 113.6, 106.2, 65.0, 13.9, 13.9, 13.3, 13.3. IR (NaCl, thin film, cm^{-1}): 3125, 2953, 2924, 2889, 2855, 1722, 1715, 1622, 1587, 1495, 1445, 1398, 1362, 1279, 1233, 1198, 1132, 1076, 1016, 988, 928, 816, 775. HRMS (ESI-TOF) m/z: $[M + H]^+$ Calcd for $C_{14}H_{14}ClO_3$265.0626; Found, 265.0618.

*4-Nitrobenzyl 2,5-Dimethylfuran-3-carboxylate (**2e**).* Synthesized according to method IV, furnishing the new compound in 32% (0.05 mmol, 0.01 g) isolated yield as a white solid, melting point: 94.8−96.5 °C, R_f 0.6 (20% ethyl acetate in hexane). ^1H NMR (400 MHz, $CDCl_3$): δ 8.26−8.20 (m, 2H), 7.58−7.52 (m, 2H), 6.24 (d, J = 0.9 Hz, 1H), 5.34 (s, 2H), 2.53 (s, 3H), 2.25 (d, J = 0.6 Hz, 3H). $^{13}C\{^1H\}$ NMR (100 MHz, $CDCl_3$): δ 163.8, 158.7, 150.5, 147.8, 143.9, 128.3, 124.0, 113.3, 106.1, 64.4, 13.9, 13.3. IR (KBr pellet, cm^{-1}): 3111, 3076, 2926, 2851, 1707, 1624, 1605, 1589, 1520, 1495, 1447, 1404, 1364, 1346, 1292, 1234, 1213, 1094, 999, 841, 775, 739. HRMS (ESI-TOF) m/z: $[M + H]^+$ Calcd for $C_{14}H_{14}NO_5$ 276.0866; Found, 276.0858.

*Octyl 2,5-Dimethylfuran-3-carboxylate (**2f**).* Synthesized according to method IV, furnishing the new compound in 85% (0.26 mmol, 0.065 g) isolated yield as a yellow oil, R_f 0.67 (20% ethyl acetate in hexane). ^1H NMR (400 MHz, $CDCl_3$): δ 6.21 (s, 1H), 4.19 (t, J = 6.7 Hz, 2H), 2.52 (s, 3H), 2.23 (s, 3H), 1.74−1.64 (m, 2H), 1.44−1.22 (m, 10H), 0.88 (t, J = 6.9 Hz, 3H). $^{13}C\{^1H\}$ NMR (100 MHz, $CDCl_3$): δ 164.6, 157.6, 150.0, 114.2, 106.4, 64.3, 31.9, 29.4, 29.3, 28.9, 26.2, 22.8, 14.2, 13.8, 13.3. IR (KBr, thin film, cm^{-1}): 2955, 2926, 2857, 1715, 1624, 1589, 1456, 1420, 1404, 1366, 1281, 1231, 1204, 1132, 1084, 777. HRMS (ESI-TOF) m/z: $[M + H]^+$ Calcd for $C_{15}H_{25}O_3$, 253.1804; Found, 253.1813.

*Decan-2-yl 2,5-Dimethylfuran-3-carboxylate (**2g**).* Synthesized according to method IV, furnishing the new compound in 83% (0.25 mmol, 0.069 g) isolated yield as a yellow oil, R_f 0.66 (10% ethyl acetate in hexane). ^1H NMR (400 MHz, $CDCl_3$): δ 6.21 (d, J = 1.1 Hz, 1H), 5.11−4.99 (m, 1H), 2.52 (s, 3H), 2.24 (dd, J = 1.1, 0.5 Hz, 3H), 1.65−1.52 (m, 2H), 1.30−1.23 (m, 15H), 0.90−0.85 (m, 3H). $^{13}C\{^1H\}$ NMR (100 MHz, $CDCl_3$): δ 164.2, 157.5, 14.9, 114.5, 106.4, 70.7, 36.2, 32.0, 29.7, 29.5, 25.6, 22.8, 20.3, 14.3, 13.9, 13.3. IR (NaCl, thin film, cm^{-1}): 2951, 2924, 2855, 1713, 1624, 1589, 1462, 1416, 1400, 1371, 1281, 1231, 1207, 1126, 1078, 1007, 986, 926, 814, 777. HRMS (ESI-TOF) m/z: $[M + H]^+$ Calcd for $C_{17}H_{29}O_3$281.2111; Found, 281.2117.

*tert-Butyl 2,5-Dimethylfuran-3-carboxylate (**2h**).*[64] Synthesized according to method IV, furnishing the known compound in 52% (0.16 mmol, 0.031 g) isolated yield as a yellow oil, R_f 0.78 (10% ethyl acetate in hexane). ^1H NMR (400 MHz, $CDCl_3$): δ 6.15 (d, J = 0.7 Hz, 1H), 2.48 (s, 3H), 2.21 (d, J = 0.5 Hz, 3H), 1.53 (s, 9H). $^{13}C\{^1H\}$ NMR (100 MHz, $CDCl_3$): δ 163.9, 157.0, 149.6, 115.5, 106.5, 80.3, 28.4, 13.8, 13.3. IR (NaCl, thin film, cm^{-1}): 3005, 2976, 2926, 1713, 1624, 1589, 1479, 1454, 1416, 1396, 1366, 1290, 1277, 1231, 1215, 1173, 1080, 1036, 1007, 986, 926, 843, 779.

*(1RS,2SR,5RS)-2-Isopropryl-5-methylcyclohexyl 2,5-Dimethylfuran-3-carboxylate (**2i**).* Synthesized according to method IV, furnishing the new compound in 80% (0.12 mmol, 0.034 g) isolated yield as a yellow oil, R_f 0.79 (10% ethyl acetate in hexane). ^1H NMR (400 MHz, $CDCl_3$): δ 6.22 (d, J = 0.9 Hz, 1H), 5.36 (d, J = 2.3 Hz, 1H), 2.54 (s, 3H), 2.24 (d, J = 0.6 Hz, 3H), 2.05−1.97 (m, 1H), 1.83−1.74 (m, 2H), 1.71−1.57 (m, 1H), 1.52−1.35 (m, 2H), 1.14−0.91 (m, 3H), 0.91−0.83 (m, 9H). $^{13}C\{^1H\}$ NMR (100 MHz, $CDCl_3$): δ 163.9, 157.3, 150.0, 115.0, 106.5, 70.8, 47.0, 39.4, 35.0, 29.5, 26.9, 25.6, 22.3, 21.0, 14.1, 13.3. IR (NaCl, thin film, cm^{-1}): 3125, 2949, 2922, 2868, 2847, 1713, 1624, 1589, 1454, 1445, 1418, 1402, 1369, 1281, 1231, 1207, 1150, 1076, 1007, 988, 957, 924, 893, 835, 814, 777. HRMS (ESI-TOF) m/z: $[M + H]^+$ Calcd for $C_{17}H_{27}O_3$ 279.1955; Found, 279.1959.

*(1RS,2RS,4SR)-1,7,7-Dimethylbicyclo[2.2.1]heptan-2-yl 2,5-Dimethylfuran-3-carboxylate (**2j**).* Synthesized according to method IV, furnishing the new compound in 54% (0.08 mmol, 0.02 g) isolated yield as a yellow oil, R_f 0.38 (20% ethyl acetate in hexane). ^1H NMR (400 MHz, $CDCl_3$): δ 6.23 (d, J = 1.0 Hz, 1H), 5.01 (ddd, J = 10.0, 3.5, 2.2 Hz, 1H), 2.54 (s, 3H), 2.43 (dddd, J = 13.6, 9.9, 4.7, 3.3 Hz, 1H), 2.25 (t, J = 0.8 Hz, 3H), 2.06−1.98 (m, 1H), 1.82−1.68 (m, 1H), 1.71 (t, J = 4.5 Hz, 1H), 1.40−1.22 (m, 2H), 1.06 (dd, J = 13.0, 3.6 Hz, 1H), 0.94 (s, 3H), 0.88 (d, J = 6.6 Hz, 6H). $^{13}C\{^1H\}$ NMR (100 MHz, $CDCl_3$): δ 164.8, 157.4, 150.0, 114.5, 106.4, 79.8, 49.0, 47.9, 45.1, 37.1, 28.2, 27.5, 19.9, 19.0, 13.7, 13.3. IR (NaCl, thin film, cm^{-1}): 3123, 2953, 2926, 2880, 1722, 1713, 1705, 1626, 1589, 1454, 1416, 1402, 1393, 1362, 1300, 1285, 1231, 1207, 1140, 1115, 1076, 1007, 989, 926, 812, 777. HRMS (ESI-TOF) m/z: $[M + H]^+$ Calcd for $C_{17}H_{25}O_3$ 277.1798; Found, 277.1787.

*(3S,8S,9S,10R,13R,14S,17R)-10,13-Dimethyl-17-((R)-6-methylheptan-2-yl)-2,3,4,7,8,9,10,11,12,13,14,15,16,17-tetradecahydro-1H-cyclopenta[a]phenanthren-3-yl 2,5-Dimethylfuran-3-carboxylate (**2k**).* Synthesized according to method IV, furnishing the new compound in 73% (0.22 mmol, 0.11 g) isolated yield as a white solid, melting point: 135.1−137.4 °C, R_f 0.9 (10% ethyl acetate in hexane), $[\alpha]_D^{25}$−7.7 (c 0.5, AcOEt). ^1H NMR (400 MHz, $CDCl_3$): δ 6.21 (d, J = 1.0 Hz, 1H), 5.40 (d, J = 5.0 Hz, 1H), 4.79−4.69 (m, 1H), 2.51 (s, 3H), 2.23 (s, 3H), 2.10−1.60 (m, 8H), 1.55−0.95 (m, 23H), 0.92 (d, J = 6.5 Hz, 3H), 0.86 (dd, J = 6.6, 1.8 Hz, 6H), 0.68 (s, 3H). $^{13}C\{^1H\}$ NMR (100 MHz, $CDCl_3$): δ 163.9, 157.6, 149.9, 139.9, 122.8, 114.4, 106.4, 73.7, 56.9, 56.3, 50.2, 42.5, 39.9, 39.7, 38.5, 37.2, 36.8, 36.3, 36.0, 32.1, 32.0, 28.4, 28.2, 24.4, 24.0, 23.0, 22.7, 22.2, 19.5, 18.9, 13.9, 13.3, 12.0. IR (KBr pellet, cm^{-1}): 2961, 2945, 2920, 2886, 2870, 2839, 1717, 1584, 1468, 1418, 1377, 1362, 1267, 1229, 1200, 1132,

https://dx.doi.org/10.1021/acs.joc.0c02777
J. Org. Chem. 2021, 86, 3923−3942

1078, 1070, 995, 820, 773. HRMS (ESI-TOF) m/z: $[M + NH_4]^+$ Calcd for $C_{34}H_{56}O_3N$ 526.4255; Found, 526.4268.

*Ethyl 2-Benzoylpent-4-enoate (**3a**).*[40] Synthesized according to method I, furnishing the known compound in 60% (3 mmol, 0.7 g) isolated yield as a translucent oil, R_f 0.49 (10% ethyl acetate in hexane). ^{1}H NMR (400 MHz, $CDCl_3$): δ 8.00−7.96 (m, 2H), 7.60−7.54 (m, 1H), 7.50−7.42 (m, 2H), 5.81 (ddt, J = 17.0, 10.2, 6.9 Hz, 1H), 5.10 (dq, J = 17.1, 1.5 Hz, 1H), 5.02 (dq, J = 10.2, 1.1 Hz, 1H), 4.39 (t, J = 7.2 Hz, 1H), 4.19−4.06 (m, 2H), 2.81−2.68 (m, 2H), 1.15 (t, J = 7.1 Hz, 3H). ^{13}C{^{1}H} NMR (100 MHz, $CDCl_3$): δ 194.6, 169.5, 136.3, 134.6, 133.6, 128.8, 128.7, 117.5, 61.5, 54.0, 33.1, 14.1. IR (NaCl, thin film, cm^{-1}): 3078, 2982, 2936, 2909, 2872, 1738, 1682, 1643, 1597, 1582, 1449, 1368, 1269, 1236, 1196, 1165, 1117, 1026, 1001, 920, 856, 779, 737, 691.

*2-(4-Nitrobenzoyl) Ethyl Pent-4-enoate (**3b**).* Synthesized according to method I, furnishing the new compound in 56% (2.8 mmol, 0.76 g) isolated yield as a yellow solid, melting point: 40.4−43.6 °C, R_f 0.63 (10% ethyl acetate in hexane). ^{1}H NMR (400 MHz, DMSO): δ 8.40−8.33 (m, 2H), 8.23−8.16 (m, 2H), 5.79 (ddt, J = 17.0, 10.2, 6.8 Hz, 1H), 5.09−4.97 (m, 2H), 4.85 (t, J = 7.0 Hz, 1H), 4.05 (q, J = 7.1 Hz, 2H), 2.62 (t, J = 7.1 Hz, 2H), 1.06 (t, J = 7.1 Hz, 3H). ^{13}C{^{1}H} NMR (100 MHz, DMSO): δ 194.6, 168.8, 150.2, 140.5, 134.5, 129.9, 124.1, 117.6, 61.2, 53.0, 39.5, 32.4, 13.9. IR (KBr pellet, cm^{-1}): 3117, 3090, 2978, 2926, 2870, 1717, 1697, 1636, 1607, 1530, 1470, 1437, 1410, 1369, 1352, 1329, 1300, 1265, 1234, 1213, 1173, 1159, 1119, 1026, 1007, 916, 854, 723. HRMS (ESI-TOF) m/z: $[M + H]^+$ Calcd for $C_{14}H_{16}NO_5$278.1023; Found, 278.1018.

*2-(3-Methoxybenzoyl) Ethyl Pent-4-enoate (**3c**).* Synthesized according to method I, furnishing the new compound in 97% (1.9 mmol, 0.51 g) isolated yield as a yellow oil, R_f 0.55 (10% ethyl acetate in hexane). ^{1}H NMR (400 MHz, $CDCl_3$): δ 7.58−7.55 (m, 1H), 7.50−7.49 (m, 1H), 7.39−7.34 (m, 1H), 7.11 (ddd, J = 8.2, 2.7, 0.9 Hz, 1H), 5.80 (ddt, J = 17.1, 10.2, 6.9 Hz, 1H), 5.01 (dq, J = 17.1, 1.6 Hz, 1H), 5.02 (dq, J = 10.3, 1.1 Hz, 1H), 4.36 (t, J = 7.2 Hz, 1H), 4.19−4.07 (m, 2H), 3.83 (s, 3H), 2.76−2.71 (m, 2H), 1.16 (t, J = 7.1 Hz, 3H). ^{13}C{^{1}H} NMR (100 MHz, $CDCl_3$): δ 194.4, 169.5, 160.0, 137.6, 134.6, 129.8, 121.3, 120.3, 117.5, 112.8, 61.5, 55.5, 54.1, 33.1, 14.1. IR (NaCl, thin film, cm^{-1}): 3078, 2980, 2940, 2837, 1738, 1688, 1643, 1597, 1584, 1487, 1464, 1450, 1431, 1368, 1323, 1265, 1229, 1182, 1117, 1042, 995, 922, 789. HRMS (ESI-TOF) m/z: $[M + H]^+$ Calcd for $C_{15}H_{19}O_4$ 263.1278; Found, 263.1275.

*Ethyl 2-Propionylpent-4-enoate (**3d**).*[65] Synthesized according to method I, furnishing the known compound in 25% (1.2 mmol, 0.22 g) isolated yield as a translucent oil, R_f 0.49 (10% ethyl acetate in hexane). ^{1}H NMR (400 MHz, $CDCl_3$): δ 5.71 (ddt, J = 17.1, 10.2, 6.9 Hz, 1H), 5.06 (dq, J = 17.1, 1.6 Hz, 1H), 5.01 (dq, J = 10.1, 1.2 Hz, 1H), 4.16 (q, J = 7.0 Hz, 2H), 3.52 (t, J = 7.4 Hz, 1H), 2.64−2.42 (m, 4H), 1.24 (t, J = 7.1 Hz, 3H), 1.04 (t, J = 7.2 Hz, 3H). ^{13}C{^{1}H} NMR (100 MHz, $CDCl_3$): δ 205.7, 169.8, 134.8, 117.8, 61.8, 58.7, 35.9, 32.7, 14.5, 8.0. IR (NaCl, thin film, cm^{-1}): 3080 2982, 2940, 2909, 2882, 1746, 1715, 1643, 1462, 1445, 1412, 1369, 1335, 1267, 1229, 1182, 1126, 1103, 1032, 999, 920, 856.

*Ethyl 2-Isobutyrylpent-4-enoate (**3e**).* Synthesized according to method I, furnishing the new compound in 45% (1.1 mmol, 0.22 g) isolated yield as a pale-yellow oil, R_f 0.66 (10% ethyl acetate in hexane). ^{1}H NMR (400 MHz, $CDCl_3$): δ 5.70 (ddt, J = 17.0, 10.1, 6.8 Hz, 1H), 5.07 (dq, J = 17.0, 1.5 Hz, 1H), 5.01 (dq, J = 10.1, 1.1 Hz, 1H), 4.18−4.13 (m, 2H), 3.68 (t, J = 7.4 Hz, 1H), 2.77 (sept, J = 6.9 Hz, 1H), 2.59−2.54 (m, 2H), 1.24 (t, J = 7.1 Hz, 3H), 1.12−1.06 (m, 6H). ^{13}C{^{1}H} NMR (100 MHz, $CDCl_3$): δ 208.5, 169.3, 134.6, 117.5, 61.4, 56.7, 40.8, 32.6, 18.4, 14.2. IR (NaCl, thin film, cm^{-1}): 3080, 2976, 2936, 2876, 1744, 1715, 1643, 1468, 1447, 1385, 1368, 1335, 1298, 1258, 1229, 1184, 1126, 1096, 1032, 1003, 920, 858. HRMS (ESI-TOF) m/z: $[M + H]^+$ Calcd for $C_{11}H_{19}O_3$199.1329; Found, 199.1326.

*Ethyl 2-(Cyclopropanocarbonyl) Pent-4-enoate (**3f**).*[66] Synthesized according to method I, furnishing the known compound in 10% (0.46 mmol, 0.091 g) isolated yield as a pale-yellow oil, R_f 0.46 (10% ethyl acetate in hexane). ^{1}H NMR (400 MHz, $CDCl_3$): δ 5.75 (ddt, J = 17.0, 10.2, 6.8 Hz, 1H), 5.09 (dq, J = 17.1, 1.6 Hz, 1H), 5.03 (dq, J = 10.2, 1.1 Hz, 1H), 4.26−4.13 (m, 2H), 3.65 (t, J = 7.4 Hz, 1H), 2.64−2.59 (m, 2H), 2.06 (tt, J = 7.8, 4.5 Hz, 1H), 1.25 (t, J = 7.1 Hz, 3H), 1.09−1.05 (m, 2H), 0.95−0.89 (m, 2H). ^{13}C{^{1}H} NMR (100 MHz, $CDCl_3$): δ 204.8, 169.5, 134.5, 117.4, 61.4, 59.6, 32.3, 20.0, 14.3, 12.0. IR (NaCl, thin film, cm^{-1}): 3080, 3007, 2982, 2938, 1738, 1703, 1643, 1445, 1420, 1383, 1337, 1298, 1263, 1229, 1180, 1132, 1078, 1045, 1011, 918, 856.

*Ethyl 2-Pivaloyl Pent-4-enoate(**3g**).* Synthesized according to method I, furnishing the new compound in 35% (1.8 mmol, 0.37 g) isolated yield as a pale-yellow oil, R_f 0.61 (10% ethyl acetate in hexane). ^{1}H NMR (400 MHz, $CDCl_3$): δ 5.70 (ddt, J = 17.1, 10.1, 7.0 Hz, 1H), 5.07 (dq, J = 17.1, 1.5 Hz, 1H), 5.02−4.98 (m, 1H), 4.17−4.07 (m, 2H), 3.94 (t, J = 7.2 Hz, 1H), 2.64−2.56 (m, 1H), 2.53−2.44 (m, 1H), 1.22 (t, J = 7.1 Hz, 3H), 1.15 (s, 9H). ^{13}C{^{1}H} NMR (100 MHz, $CDCl_3$): δ 209.4, 169.3, 134.9, 117.5, 61.4, 52.4, 45.3, 34.1, 26.2, 14.2. IR (NaCl, thin film, cm^{-1}): 3080, 2976, 2938, 2909, 2874, 1746, 1709, 1643, 1479, 1466, 1441, 1395, 1368, 1327, 1271, 1225, 1182, 1119, 1059, 1026, 997, 959, 918. HRMS (ESI-TOF) m/z: $[M + H]^+$ Calcd for $C_{12}H_{21}O_3$213.1485; Found, 213.1483.

*2-(2-Methoxyacetyl) Methyl Pent-4-enoate (**3h**).* Synthesized according to method I, furnishing the new compound in 43% (1.1 mmol, 0.19 g) isolated yield as a translucent oil, R_f 0.24 (10% ethyl acetate in hexane). ^{1}H NMR (400 MHz, $CDCl_3$): δ 5.71 (ddt, J = 17.1, 10.1, 6.9 Hz, 1H), 5.06 (dq, J = 17.0, 1.6 Hz, 1H), 5.01 (dq, J = 10.2, 1.1 Hz, 1H), 4.09 (d, J = 17.0 Hz, 1H), 4.04 (d, J = 17.0 Hz, 1H), 3.70−3.65 (m, 4H), 3.37 (s, 3H), 2.60−2.55 (m, 2H). ^{13}C{^{1}H} NMR (100 MHz, $CDCl_3$): δ 202.9, 169.3, 134.0, 117.6, 76.7, 59.3, 54.1, 52.3, 31.7. IR (NaCl, thin film, cm^{-1}): 3080, 2986, 2953, 2828, 1748, 1732, 1717, 1643, 1454, 1435, 1339, 1269, 1233, 1200, 1121, 995, 922. HRMS (ESI-TOF) m/z: $[M + H]^+$ Calcd for $C_9H_{15}O_4$187.0965; Found, 187.0965.

*Ethyl 5-Methyl-2-phenylfuran-3-carboxylate(**4a**).*[67] Synthesized according to method IV, furnishing the known compound in 67% (0.20 mmol, 0.044 g) isolated yield as a translucent oil, R_f 0.62 (10% ethyl acetate in hexane). ^{1}H NMR (400 MHz, $CDCl_3$): δ 7.98−7.94 (m, 2H), 7.45−7.34 (m, 3H), 6.44 (q, J = 1.0 Hz, 1H), 4.28 (q, J = 7.1 Hz, 2H), 2.35 (d, J = 1.1 Hz, 3H), 1.32 (t, J = 7.1 Hz, 3H). ^{13}C{^{1}H} NMR (100 MHz, $CDCl_3$): δ 163.9, 156.0, 151.2, 130.2, 129.0, 128.2, 128.1, 114.6, 108.9, 60.5, 14.4, 13.5. IR (NaCl, thin film, cm^{-1}): 3075, 3057, 3032, 2982, 2924, 2905, 2872, 1722, 1715, 1614, 1603, 1580, 1557, 1493, 1447, 1412, 1379, 1290, 1273, 1209, 1134, 1096, 1040, 1024, 1003, 986, 918, 831, 781, 762, 692.

*Ethyl 5-Methyl-2-(4-nitrophenyl)furan-3-carboxylate(**4b**).*[68] Synthesized according to method IV, furnishing the known compound in 47% (0.14 mmol, 0.038 g) isolated yield as a yellow solid, mp 77,3−79,2 °C, R_f 0.63 (20% ethyl acetate in hexane). ^{1}H NMR (400 MHz, DMSO): δ 8.21−8.26 (m, 2H), 8.18−8.14 (m, 2H), 6.59 (d, J = 0.9 Hz, 1H), 4.24 (q, J = 7.1 Hz, 2H), 2.37 (s, 3H), 1.26 (t, J = 7.1 Hz, 3H). ^{13}C{^{1}H} NMR (100 MHz, DMSO): δ 162.6, 153.6, 151.9, 147.0, 135.1, 128.5, 123.6, 117.2, 109.7, 60.7, 39.5, 14.0, 13.1. IR (KBr pellet, cm^{-1}): 3100, 3076, 3011, 2988, 1722, 1715, 1597, 1568, 1516, 1489, 1449, 1404, 1379, 1354, 1300, 1281, 1260, 1215, 1132, 1094, 1028, 999, 991, 854, 829, 812, 773, 752, 694.

*Ethyl 2-(3-Methoxyphenyl)-5-methylfuran-3-carboxylate (**4c**).* Synthesized according to method IV, furnishing the new compound in 67% (0.20 mmol, 0.051 g) isolated yield as a white oil, R_f 0.53 (10% ethyl acetate in hexane). ^{1}H NMR (400 MHz, $CDCl_3$): δ 7.62−7.54 (m, 2H), 7.32 (t, J = 8.0 Hz, 1H), 6.92 (ddd, J = 8.3, 2.6, 0.9 Hz, 1H), 6.44 (q, J = 1.0 Hz, 1H), 4.28 (q, J = 7.1 Hz, 2H), 3.86 (s, 3H), 2.35 (d, J = 1.0 Hz, 3H), 1.33 (t, J = 7.1 Hz, 3H). ^{13}C{^{1}H} NMR (100 MHz, $CDCl_3$): δ 163.9, 159.4, 155.7, 151.1, 131.3, 129.1, 120.6, 115.1, 114.8, 113.4, 109.0, 60.5, 55.5, 14.4 13.5. IR (NaCl, thin film, cm^{-1}): 3121, 3080, 2980, 2957, 2940, 2907, 2835, 1721, 1715, 1605, 1557, 1493, 1464, 1454, 1435, 1377, 1317, 1292, 1281, 1256, 1211, 1180, 1134, 1098, 1047, 1032, 860, 820, 775, 698. HRMS (ESI-TOF) m/z: $[M + H]^+$ Calcd for $C_{15}H_{17}O_4$261.1121; Found, 261.1109.

*Ethyl 2-Ethyl-5-methylfuran-3-carboxylate(**4d**).* Synthesized according to method IV, furnishing the new compound in 56% (0.17 mmol, 0.030 g) isolated yield as a yellow oil, R_f 0.68 (10% ethyl acetate in hexane). ^{1}H NMR (400 MHz, $CDCl_3$): δ 6.20 (d, J = 1.1

https://dx.doi.org/10.1021/acs.joc.0c02777
J. Org. Chem. 2021, 86, 3923−3942

Hz, 1H), 4.25 (q, J = 7.1 Hz, 2H), 2.94 (q, J = 7.6 Hz, 2H), 2.23 (d, J = 1.1 Hz, 3H), 1.32 (t, J = 7.1 Hz, 3H), 1.22 (t, J = 7.6 Hz, 3H). $^{13}C\{^1H\}$ NMR (100 MHz, $CDCl_3$): δ 164.4, 162.7, 150.0, 113.2, 106.3, 60.0, 21.3, 14.5, 13.3, 12.5. IR (NaCl, thin film, cm^{-1}): 2980, 2938, 2928, 2880, 1715, 1620, 1584, 1464, 1418, 1402, 1385, 1304, 1252, 1204, 1136, 1088, 1043, 962, 945, 837, 779. HRMS (ESI-TOF) m/z: $[M + H]^+$ Calcd for $C_{10}H_{15}O_3$183.1016; Found, 183.1017.

*Ethyl 2-Isopropyl-5-methylfuran-3-carboxylate(**4e**).*[47] Synthesized according to method IV, furnishing the known compound in 74% (0.22 mmol, 0.044 g) isolated yield as a yellow oil, R_f 0.70 (10% ethyl acetate in hexane). ^1H NMR (400 MHz, $CDCl_3$): δ 6.19 (d, J = 1.1 Hz, 1H), 4.25 (q, J = 7.1 Hz, 2H), 3.70 (sept, J = 7.0 Hz, 1H), 2.23 (d, J = 1.0 Hz, 3H), 1.32 (t, J = 7.1 Hz, 3H), 1.24 (d, J = 7.0 Hz, 6H). $^{13}C\{^1H\}$ NMR (100 MHz, $CDCl_3$): δ 165.8, 164.4, 149.7, 119.3, 106.2, 60.0, 27.2, 20.9, 14.5, 13.3.

*Ethyl 2-Cyclopropyl-5-methylfuran-3-carboxylate (**4f**).* Synthesized according to method IV, furnishing the new compound in 60% (0.20 mmol, 0.041 g) isolated yield as an off-white solid, mp 54,7−58 °C, R_f 0.68 (10% ethyl acetate in hexane). ^1H NMR (400 MHz, DMSO): δ 6.22 (s, 1H), 4.20 (q, J = 7.1 Hz, 2H), 2.68−2.61 (m, 1H), 2.16 (s, 3H), 1.25 (t, J = 7.1 Hz, 3H), 1.05−0.87 (m, 4H). $^{13}C\{^1H\}$ NMR (100 MHz, $CDCl_3$): δ 163.5, 160.8, 149.0, 113.1, 106.3, 59.6, 14.3, 12.8, 8.9, 8.2. IR (KBr pellet, cm^{-1}): 3123, 3098, 3063, 3017, 2992, 2978, 2949, 2924, 2907, 1697, 1645, 618, 1584, 1479, 1408, 1387, 1339, 1285, 1244, 1202, 1180, 1067, 1057, 1024, 947, 887, 826, 808, 783. HRMS (ESI-TOF) m/z: $[M + H]^+$ Calcd for $C_{11}H_{15}O_3$195.1016; Found, 195.1017.

*Ethyl 2-(tert-Butyl)-5-methylfuran-3-carboxylate (**4g**).*[69] Synthesized according to method IV, furnishing the known compound in <2% isolated yield as a yellow oil, R_f 0.75 (10% ethyl acetate in hexane). ^1H NMR (400 MHz, $CDCl_3$): δ 6.26 (d, J = 1.0 Hz, 1H), 4.25 (q, J = 7.1 Hz, 2H), 2.23 (d, J = 1.1 Hz, 3H), 1.40 (s, 9H), 1.33 (t, J = 7.1 Hz, 3H). IR (NaCl, thin film, cm^{-1}): 2976, 2959, 2930, 2907, 2872, 1721, 1715, 1557, 1481, 1464, 1373, 1267, 1221, 1204, 1155, 1111, 1063, 1026, 781.

*Methyl 2-(Methoxymethyl)-5-methylfuran-3-carboxylate (**4h**).* Synthesized according to method IV, furnishing the new compound in 18% (0.05 mmol, 0.01 g) isolated yield as a yellow oil, R_f 0.39 (10% ethyl acetate in hexane). ^1H NMR (400 MHz, $CDCl_3$): δ 6.28 (d, J = 1.1 Hz, 1H), 4.69 (s, 2H), 3.82 (s, 3H), 3.40 (s, 3H), 2.29 (d, J = 1.0 Hz, 3H). $^{13}C\{^1H\}$ NMR (100 MHz, $CDCl_3$): δ 164.1, 155.4, 152.5, 117.1, 106.6, 64.9, 58.5, 51.6, 13.5. IR (NaCl, thin film, cm-^{1}) 3123, 3098, 3063, 3017, 2992, 2949, 2924, 2907, 1697, 1645, 1618, 1584, 1479, 1408, 1387, 1379, 1339, 1285, 1244, 1202, 1180, 1067, 1057, 1024, 947, 887, 833, 783. HRMS (ESI-TOF) m/z: $[M + H]^+$ Calcd for $C_9H_{13}O_4$185.0814; Found, 185.0820.

*2-Allyl-1-phenylbutane-1,3-dione (**5a**).*[70] Synthesized according to method I, furnishing the known compound in 68% (0.24 mmol, 0.049 g) isolated yield as an orange oil, R_f 0.44 (10% ethyl acetate in hexane). ^1H NMR (400 MHz, $CDCl_3$): δ 7.98 (m, 2H), 7.62−7.56 (m, 1H), 7.50−7.45 (m, 2H), 5.75 (ddt, J = 17.0, 10.2, 6.8 Hz, 1H), 5.08 (dq, J = 17.1, 1.5 Hz, 1H), 5.02 (dq, J = 10.2, 1.2 Hz, 1H), 4.54 (t, J = 7.2 Hz, 1H), 2.81−2.66 (m, 2H), 2.14 (s, 3H). $^{13}C\{^1H\}$ NMR (100 MHz, $CDCl_3$): δ 203.7, 195.9, 136.4, 134.5, 133.9, 129.0, 128.8, 117.6, 62.8, 33.1, 28.2. IR (NaCl, thin film, cm^{-1}): 3230, 3154, 3131, 3071, 1874, 1829, 1793, 1746, 1731, 1600, 1509, 1488, 1407, 1380, 1355, 1334, 1152, 1119, 1073, 930, 901, 844.

*2-Allyl-1,3-diphenylpropane-1,3-dione (**5b**).*[71] Synthesized according to method I, furnishing the known compound in 54% (0.8 mmol, 0.2 g) isolated yield as a white solid, R_f 0.49 (10% ethyl acetate in hexane). ^1H NMR (400 MHz, $CDCl_3$): δ 7.99−7.93 (m, 4H), 7.57 (td, J = 7.5, 1.3 Hz, 2H), 7.49−7.42 (m, 4H), 5.93−5.82 (m, 1H), 5.29 (dd, J = 7.3, 6.2 Hz, 1H), 5.10 (dt, J = 17.1, 1.5 Hz, 1H), 5.03 (d, J = 10.2 Hz, 1H), 2.88 (td, J = 6.8, 1.3 Hz, 2H). $^{13}C\{^1H\}$ NMR (100 MHz, $CDCl_3$): δ 195.7, 136.1, 135.2, 133.7, 129.0, 128.8, 117.4, 56.9, 33.7. IR (KBr pellet, cm^{-1}): 3082, 3063, 2932, 2913, 1694, 1667, 1593, 1578, 1447, 1331, 1269, 1234, 1207, 1173, 1003, 926, 907, 799, 760, 694, 687.

*2-Allylcyclohexane-1,3-dione (**5c**).*[72] Synthesized according to method I, furnishing the known compound in 30% (0.58 mmol, 0.089 g) isolated yield as a yellow oil, R_f 0.33 (20% ethyl acetate in hexane). ^1H NMR (400 MHz, DMSO-d_6): δ 5.97 (ddt, J = 16.4, 10.6, 5.4 Hz, 1H), [5.76−5.59 (m, 0.20H)]*, 5.44−5.12 (m, 3H), [4.86 (dd, J = 24.2, 13.6 Hz, 0.41H)]*, [4.64 (d, J = 3.8 Hz, 0.43H)]*, 4.51−4.37 (m, 2H), [3.50 (s, 0.04H)]*, [2.91 (d, J = 6.2 Hz, 0.42H)]*, [2.64 (t, J = 6.2 Hz, 0.43H)]*, 2.40 (t, J = 6.2 Hz, 2H), 2.20 (t, J = 6.4 Hz, 2H), 1.87 (p, J = 6.3 Hz, 2H). $^{13}C\{^1H\}$ NMR (100 MHz, $CDCl_3$): δ 198.1, 176.9, 132.3, 118.4, 102.7, 68.7, 36.4, 28.3, 20.9. IR (KBr, thin film, cm^{-1}): 3082, 2947, 2893, 2878, 1651, 1605, 1458, 1427, 1373, 1350, 1331, 1223, 1184, 1138, 991, 961, 930, 864, 826, 760, 498, 467.* *refers to the minor stereoisomer.*

*Benzyl (E)-2-Acetyl-3,5-diphenylpent-4-enoate (**5d**).* Synthesized according to method III, furnishing the new compound in 66% (0.3 mmol, 0.1 g) isolated yield as a white solid, mp 78.2−79.8 °C, R_f 0.69 (20% ethyl acetate in hexane). ^1H NMR (400 MHz, $CDCl_3$): δ 7.39−7.16 (m, 28 H), 7.07−6.99 (m, 2H), 6.44−6.38 (m, 2H), 6.30−6.20 (m, 2 H), 5.17 (d, J = 12.2 Hz, 1H), [5.07 (d, J = 12.1 Hz, 1H)]*, 4.96−4.84 (m, 2 H), 4.35−4.25 (m, 2 H), 4.20−4.10 (m, 2 H), 2.26 (s, 3H), [2.00 (s, 3H)]*. $^{13}C\{^1H\}$ NMR (100 MHz, $CDCl_3$): δ 201.6, 201.4, 168.0, 167.6, 140.4, 140.2, 136.8, 136.7, 135.2, 132.0, 131.7, 129.4, 129.2, 129.1, 128.9, 128.7, 128.6, 128.4, 128.3, 128.1, 127.8, 127.7, 127.3, 127.3, 126.5, 67.5, 67.3, 65.6, 65.3, 49.2, 48.9, 30.2, 30.0. IR (KBr pellet, cm^{-1}): 3080, 3059, 3026, 2963, 2953, 1734, 1711, 1597, 1495, 1454, 1381, 1366, 1288, 1279, 1211, 1186, 1148, 1092, 970, 949, 768, 748, 696. HRMS (ESI-TOF) m/z: $[M + Na]^+$ Calcd for $C_{26}H_{24}O_3Na$ 407.1623; Found, 407.1617.**the indicated signals appear duplicated in the spectrum but integrate for the correct amount of hydrogens of only one molecule and are therefore referring only to one of the diastereoisomers. The other signs correspond to twice the expected amount of hydrogens.*

*(E)-3-(1,3-Diphenylallyl)pentane-2,4-dione (**5e**).*[17] Synthesized according to method III, furnishing the known compound in 84% (0.4 mmol, 0.1 g) isolated yield as a white solid, mp 76.9−78.1 °C, R_f 0.22 (10% ethyl acetate in hexane). ^1H NMR (400 MHz, $CDCl_3$): δ 7.35−7.18 (m, 10H), 6.43 (d, J = 15.8 Hz, 1H), 6.19 (ddd, J = 15.8, 5.6, 2.3 Hz, 1H), 4.38−4.29 (m, 2H), 2.25 (s, 3H), 1.92 (s, 3H). $^{13}C\{^1H\}$ NMR (100 MHz, $CDCl_3$): δ 203.0, 202.9, 140.2, 136.6, 131.8, 129.3, 129.1, 128.6, 128.0, 127.8, 127.4, 126.5, 74.6, 49.3, 30.2, 29.9. IR (KBr pellet, cm^{-1}): 3082, 3059, 3024, 2916, 1722, 1697, 1599, 1495, 1452, 1416, 1377, 1360, 1287, 1271, 1248, 1173, 1140, 1070, 1030, 988, 974, 766, 745, 704.

*1-(5-Methyl-2-phenylfuran-3-yl)ethan-1-one (**6a**).*[73] Synthesized according to method IV, furnishing the known compound in 50% (0.06 mmol, 0.01 g) isolated yield as a yellow oil, R_f 0.72 (10% ethyl acetate in hexane). ^1H NMR (400 MHz. $CDCl_3$): δ 7.74−7.68 (m, 2H), 7.50−7.44 (m, 1H), 7.38 (dd, J = 8.2, 6.8 Hz, 2H), 6.09 (s, 1H), 2.41 (s, 3H), 2.21 (s, 3H). $^{13}C\{^1H\}$ NMR (100 MHz, $CDCl_3$): δ 171.3, 158.1, 149.9, 139.5, 132.1, 129.1, 128.4, 121.3, 107.6, 60.5, 29.8, 21.2, 14.3, 13.3. IR (NaCl, thin film, cm^{-1}): 3206, 3170, 3137, 3110, 3075, 3004, 1849, 1802, 1750, 1719, 1598, 1546, 1517, 1438, 1416, 1386, 1370, 1160, 1054, 890, 855.

*(5-Methyl-2-phenylfuran-3-yl)(phenyl)methanone (**6b**).*[16] Synthesized according to method IV, furnishing the known compound in 67% (0.2 mmol, 0.05 g) isolated yield as a yellow oil, R_f 0.68 (10% ethyl acetate in hexane). ^1H NMR (400 MHz. $CDCl_3$): δ 7.83 (d, J = 8.1 Hz, 2H), 7.66 (d, J = 7.6 Hz, 2H), 7.48 (t, J = 7.4 Hz, 1H), 7.36 (t, J = 7.6 Hz, 2H), 7.27 (m, 3H), 6.29 (s, 1H), 2.39 (s, 3H). $^{13}C\{^1H\}$ NMR (100 MHz, $CDCl_3$): δ 192.1, 154.6, 151.3, 138.3, 132.8, 130.1, 129.8, 128.7, 128.4, 127.4, 121.9, 109.9, 13.6. IR (KBr, thin film, cm^{-1}): 3059, 3028, 2955, 2920, 1655, 1597, 1578, 1551, 1489, 1447, 1373, 1315, 1277, 1223, 1177, 1126, 1072, 1015, 999, 887, 768, 725, 691, 675, 467.

*Methyl 2-Acetylpent-4-enoate (**7**).*[74] Synthesized according to method I, furnishing the known compound in 30% (6 mmol, 1 g) isolated yield as a pale-yellow oil, R_f0 .47 (10% ethyl acetate in hexane). ^1H NMR (400 MHz, $CDCl_3$): δ 5.74 (ddt, J = 17.0, 10.2, 6.8 Hz, 1H), 5.10 (dq, J = 17.1, 1.5 Hz, 1H), 5.05 (dq, J = 10.2, 1.2 Hz, 1H), 3.76−3.73 (m, 3H), 3.55 (t, J = 7.4 Hz, 1H), 2.63−2.57 (m, 2H), 2.24 (s, 3H). $^{13}C\{^1H\}$ NMR (100 MHz, $CDCl_3$): δ 202.5, 169.8, 134.3, 117.7, 59.2, 52.6, 32.3, 29.3. IR (NaCl, thin film, cm^{-1}):

https://dx.doi.org/10.1021/acs.joc.0c02777
J. Org. Chem. 2021, 86, 3923−3942

3080, 3005, 2982, 2955, 2924, 2847, 1746, 1715, 1643, 1435, 1360, 1269, 1233, 1198, 1152, 1121, 1059, 995, 922, 847.

*d_1-Benzyl 2-Acetylpent-4-enoate (**1a′**).* Synthesized according to method V, furnishing the compound in 63% (0.63 mmol, 0.15 g) isolated yield (78% of deuterium incorporated) as a yellow oil, R_f 0.33 (10% ethyl acetate in hexane) ^{1}H NMR (400 MHz. $CDCl_3$): δ 7.34−7.21 (m, 5H), 5.65 (ddt, J = 17.1, 10.2, 6.8 Hz, 1H), 5.10 (s, 2H), 5.03−4.92 (m, 2H), 3.5 (t, J = 7.4 Hz, 0.22H), 2.53 (d, J = 6.7 Hz, 2H), 2.11 (s, 3H). $^{13}C\{^1H\}$ NMR (100 MHz, $CDCl_3$): δ 202.4, 169.2, 135.4, 134.2, 128.7, 128.7, 128.6, 128.5, 117.7, 67.3, 59.3, 32.2, 29.3. IR (KBr, thin film, cm^{-1}): 3078, 3067, 3036, 2982, 2959, 2924, 1740, 1713, 1643, 1497, 1454, 1435, 1358, 1265, 1231, 1192, 1142, 1107, 1061, 995, 918, 826, 748, 698, 644, 594, 471.

■ ASSOCIATED CONTENT

Supporting Information

The Supporting Information is available free of charge at https://pubs.acs.org/doi/10.1021/acs.joc.0c02777.

Copies of ^{1}H, ^{13}C, and IV spectra, additional computational discussions, optimized geometries, and energies corresponding to all stationary points (PDF)

FAIR data, including the primary NMR FID files, for compounds **1a−k**, **1a′**, **2a−k**, **3a−h**, **4a−h**, **5a−e**, **6a,b**, **7**, and experimental compounds (ZIP)

■ AUTHOR INFORMATION

Corresponding Author

Marco A. B. Ferreira − *Centre for Excellence for Research in Sustainable Chemistry (CERSusChem), Department of Chemistry, Federal University of São Carlos - UFSCar, São Carlos, São Paulo 13565-905, Brazil;* orcid.org/0000-0002-4954-6691; Email: marco.ferreira@ufscar.br

Authors

Amanda A. Barboza − *Centre for Excellence for Research in Sustainable Chemistry (CERSusChem), Department of Chemistry, Federal University of São Carlos - UFSCar, São Carlos, São Paulo 13565-905, Brazil;* orcid.org/0000-0001-5606-911X

Attilio Chiavegatti Neto − *Centre for Excellence for Research in Sustainable Chemistry (CERSusChem), Department of Chemistry, Federal University of São Carlos - UFSCar, São Carlos, São Paulo 13565-905, Brazil;* orcid.org/0000-0002-4266-4409

Isac G. Rosset − *Centre for Excellence for Research in Sustainable Chemistry (CERSusChem), Department of Chemistry, Federal University of São Carlos - UFSCar, São Carlos, São Paulo 13565-905, Brazil; Universidade Federal do Paraná - Departamento de Engenharias e Exatas, Palotina, Paraná 85950-000, Brazil;* orcid.org/0000-0003-2989-7854

Guilherme A. M. Jardim − *Centre for Excellence for Research in Sustainable Chemistry (CERSusChem), Department of Chemistry, Federal University of São Carlos - UFSCar, São Carlos, São Paulo 13565-905, Brazil;* orcid.org/0000-0002-9882-3085

Complete contact information is available at: https://pubs.acs.org/10.1021/acs.joc.0c02777

Author Contributions

§A.A.B. and A.C.N. contributed equally to this work.

Notes

The authors declare no competing financial interest.

■ ACKNOWLEDGMENTS

The authors gratefully acknowledge FAPESP (Grant Nos. 2014/50249-8, 2020/10246-0, and 2020/01255-6), GlaxoSmithKline, CAPES (Finance Code 001), and PNPD/CAPES and CNPq for funding and fellowships. We thank Prof. Cláudio F. Tormena for the computational facilities.

■ REFERENCES

(1) A critical review of the 2002 literature preceded by three chapters on current heterocyclic topics: Hou, X.-L.; Yang, Z.; Wong, H. N. C. Chapter 5.3 Five-Membered Ring Systems: Furans and Benzofurans. In *Progress in Heterocyclic Chemistry*; Gribble, G. W., Joule, J. A., Eds.; Elsevier, 2003; Vol. *15*, pp 167−205.

(2) Lipshutz, B. H. Five-Membered Heteroaromatic Rings as Intermediates in Organic Synthesis. *Chem. Rev.* **1986**, *86*, 795−819.

(3) Baumann, M.; Baxendale, I. R.; Ley, S. V.; Nikbin, N. An overview of the key routes to the bestselling 5-membered ring heterocyclic pharmaceuticals. *Beilstein J. Org. Chem.* **2011**, *7*, 442−495.

(4) Kapojos, M. M.; Lee, J.-S.; Oda, T.; Nakazawa, T.; Takahashi, O.; Ukai, K.; Mangindaan, R. E. P.; Rotinsulu, H.; Wewengkang, D. S.; Tsukamoto, S.; Kobayashi, H.; Namikoshi, M. Two unprecedented cembrene-type terpenes from an indonesian soft coral sarcophyton sp. *Tetrahedron* **2010**, *66*, 641−645.

(5) Guo, Y.; Quan, T.; Lu, Y.; Luo, T. Enantioselective Total Synthesis of (+)-Wortmannin. *J. Am. Chem. Soc.* **2017**, *139*, 6815−6818.

(6) Yu, Y.; Zheng, J.; Cao, L.; Li, S.; Li, X.; Zhou, H.-B.; Liu, X.; Wu, S.; Dong, C. Furan-carboxamide derivatives as novel inhibitors of lethal H5N1 influenza A viruses. *RSC Adv.* **2017**, *7*, 9620−9627.

(7) (a) Ma, S.; Yu, Z. Oxidative Cyclization-Dimerization Reaction of 2,3-Allenoic Acids and 1,2-Allenyl Ketones: An Efficient Synthesis of 4-(3′-Furanyl)butenolide Derivatives. *Angew. Chem.* **2002**, *114*, 1853−1856. (b) Ma, S.; Zhang, J.; Lu, L. Pd(0)-Catalyzed Coupling Cyclization Reaction of Aryl or Alkenyl Halides with 1,2-Allenyl Ketones: Scope and Mechanism. *Chem. - Eur. J.* **2003**, *9* (11), 2447−2456. (c) Xiao, Y.; Zhang, J. Palladium(II)-Catalyzed Domino Reaction of 2-(1-Alkynyl)-2-alken-1-ones with Nucleophiles: Scope, Mechanism and Synthetic Application in the Synthesis of 3,4-Fused Bicyclic Tetrasubstituted Furans. *Adv. Synth. Catal.* **2009**, *351*, 617−629. (d) Cheng, C.; Liu, S.; Zhu, G. Palladium-Catalyzed Cycloisomerization and Aerobic Oxidative Cycloisomerization of Homoallenyl Amides: A Facile and Divergent Approach to 2-Aminofurans. *Org. Lett.* **2015**, *17*, 1581−1584. (e) Duc, D. X. Recent Progress in the Synthesis of Furan. *Mini-Rev. Org. Chem.* **2019**, *16*, 422−452.

(8) Zeni, G.; Larock, R. C. Synthesis of Heterocycles via Palladium π-Olefin and π-Alkyne Chemistry. *Chem. Rev.* **2004**, *104*, 2285−2310.

(9) McDonald, R. I.; Liu, G.; Stahl, S. S. Palladium(II)-Catalyzed Alkene Functionalization via Nucleopalladation: Stereochemical Pathways and Enantioselective Catalytic Applications. *Chem. Rev.* **2011**, *111*, 2981−3019.

(10) Campbell, A. N.; Stahl, S. S. Overcoming the "Oxidant Problem": Strategies to Use O2 as the Oxidant in Organometallic C-H Oxidation Reactions Catalyzed by Pd (and Cu). *Acc. Chem. Res.* **2012**, *45*, 851−863.

(11) Barton, D. H. R; Martell, A. E.; Sawyer, D. T. *The Activation of Dioxygen and Homogeneous Catalytic Oxidation*; Plenum Press: New York, 1993.

(12) Konnick, M. M.; Gandhi, B. A.; Guzei, I. A.; Stahl, S. S. Reaction of Molecular Oxygen with a PdII- Hydride to Produce a PdII-Hydroperoxide: Acid Catalysis and Implications for Pd-Catalyzed Aerobic Oxidation Reactions. *Angew. Chem., Int. Ed.* **2006**, *45*, 2904−2907.

(13) Beccalli, E. M.; Broggini, G.; Martinelli, M.; Sottocornola, S. C-C, C-O, C-N Bond Formation on sp2 Carbon by Pd(II)-Catalyzed Reactions Involving Oxidant Agents. *Chem. Rev.* **2007**, *107*, 5318−5365.

(14) (a) Steinhoff, B. A.; King, A. E.; Stahl, S. S. Unexpected Roles of Molecular Sieves in Palladium-Catalyzed Aerobic Alcohol Oxidation. *J. Org. Chem.* **2006**, *71*, 1861−1868. (b) Nishimura, T.; Maeda, Y.; Kakiuchi, N.; Uemura, S. Palladium(II)-catalysed oxidation of alcohols under an oxygen atmosphere in a fluorous biphase system (FBS). *J. Chem. Soc., Perkin Trans. 1* **2000**, 4301−4305.
(15) Wang, D.; Weinstein, A. B.; White, P. B.; Stahl, S. S. Ligand-Promoted Palladium-Catalyzed Aerobic Oxidation Reactions. *Chem. Rev.* **2018**, *118*, 2636−2679.
(16) Gligorich, K. M.; Sigman, S. S. Recent advancements and challenges of palladium(II)-catalyzed oxidation reactions with molecular oxygen as the sole oxidant. *Chem. Commun.* **2009**, 3854−3867.
(17) Jensen, D. R.; Pugsley, J. S.; Sigman, M. S. Palladium-Catalyzed Enantioselective Oxidations of Alcohols Using Molecular Oxygen. *J. Am. Chem. Soc.* **2001**, *123*, 7475−7476.
(18) Trend, R. M.; Ramtohul, Y. K.; Ferreira, E. M.; Stoltz, B. M. Palladium-Catalyzed Oxidative Wacker Cyclizations in Nonpolar Organic Solvents with Molecular Oxygen: A Stepping Stone to Asymmetric Aerobic Cyclizations. *Angew. Chem., Int. Ed.* **2003**, *42*, 2892−2895.
(19) (a) Arcadi, A.; Rossi, E. A Palladium - Catalyzed Domino Reaction of 3-Acetyl-5-hexyn-2-one with Aryl Iodides under Carbon Monoxide. *Tetrahedron Lett.* **1996**, *37*, 6811−6814. (b) Arcadi, A.; Cacchi, S.; Fabrizi, G.; Marinelli, F.; Parisi, L. M. Highly substituted furans from 2-propynyl-1,3-dicarbonyls and organic halides or triflates via the oxypalladation-reductive elimination domino reaction. *Tetrahedron* **2003**, *59*, 4661−4671. (c) Saito, A.; Enomoto, Y.; Hanzawa, Y. Pd-catalyzed cycloisomerization-allylation of 4-alkynones: synthesis of 5-homoallylfuran derivatives. *Tetrahedron Lett.* **2011**, *52*, 4299−4302. (d) Ruengsangtongkul, S.; Chaisan, N.; Thongsornkleeb, C.; Tummatorn, J.; Ruchirawat, S. Rate Enhancement in CAN-Promoted Pd(PPh3)2Cl2-Catalyzed Oxidative Cyclization: Synthesis of 2-Ketofuran-4-carboxylate Esters. *Org. Lett.* **2019**, *21*, 2514−2517.
(20) Han, X.; Widenhoefer, R. A. Palladium-Catalyzed Oxidative Alkoxylation of α-Alkenyl β-Diketones to Form Functionalized Furans. *J. Org. Chem.* **2004**, *69*, 1738−1740.
(21) (a) Nallagonda, R.; Reddy, R. R.; Ghorai, P. Palladium-Catalyzed Oxidative Cycloisomerization of 2-Cinnamyl-1,3-Dicarbonyls: Synthesis of Functionalized 2-Benzyl Furans. *Chem. - Eur. J.* **2015**, *21*, 14732−14736. (b) Rehan, M.; Nallagonda, R.; Das, B. G.; Meena, T.; Ghorai, P. Synthesis of Functionalized Benzo[b]furans via Oxidative Cyclization of o-Cinnamyl Phenols. *J. Org. Chem.* **2017**, *82*, 3411−3424.
(22) (a) Ali, S.; Milanezi, H.; Alves, T. M. F.; Tormena, C. F.; Ferreira, M. A. B. Cobalt-catalysed Stereoselective Synthesis of 2,5-trans-THF Nitrile Derivatives as a Platform for Diversification: Development and Mechanistic Studies. *J. Org. Chem.* **2018**, *83*, 7694−7713. (b) Alves, T. M. F.; Costa, M. O.; Bispo, B. A. D.; Pedrosa, F. L.; Ferreira, M. A. B. Cobalt-catalyzed oxidative cyclization of gem-disubstituted conjugated alkenols. *Tetrahedron Lett.* **2016**, *57*, 3334−3338.
(23) (a) Shanker, K.; Reddy, P. M.; Rohini, R.; Ho, Y.; Ravinder, V. Encapsulation of Pd(II) by N4 and N2O2 macrocyclic ligands: their use in catalysis and biology. *J. Coord. Chem.* **2009**, *62*, 3040−3049. (b) Aghayee, M.; Zolfigol, M. A.; Keypour, H.; Yarie, M.; Mohammadi, L. Synthesis and characterization of a novel magnetic nano-palladium Schiff base complex: application in cross-coupling reactions. *Appl. Organomet. Chem.* **2016**, *30*, 612−618. (c) Movassagh, B.; Ranjbari, S. Kryptofix 5 as an inexpensive and efficient ligand for the palladium-catalyzed Mizoroki-Heck reaction. *Appl. Organomet. Chem.* **2018**, *32*, 1−12.
(24) Luyckx, G.; Ceulemans, J. Deoxygenation, Deaeration and Degassing: A Survey and Evaluation of Methods. *Bull. Soc. Chim. Belg.* **1987**, *96*, 151−163.
(25) Keith, J. A.; Henry, P. M. The Mechanism of the Wacker Reaction: A Tale of Two Hydroxypalladations. *Angew. Chem., Int. Ed.* **2009**, *48*, 9038−9049.
(26) (a) Eisenstein, O.; Hoffmann, R. Activation of a coordinated olefin toward nucleophilic attack. *J. Am. Chem. Soc.* **1980**, *102*, 6148−6149. (b) Eisenstein, O.; Hoffmann, R. Transition-metal complexed olefins: how their reactivity toward a nucleophile relates to their electronic structure. *J. Am. Chem. Soc.* **1981**, *103*, 4308−4320.
(27) (a) Åkermark, B.; Bäckvall, J. E.; Hegedus, L. S.; Zetterberg, K.; Siirala-Hansén, K.; Sjöberg, K. Palladium-promoted addition of amines to isolated double bonds. *J. Organomet. Chem.* **1974**, *72*, 127−138. (b) Timokhin, V. I.; Stahl, S. S. Bronsted base-modulated regioselectivity in the aerobic oxidative amination of styrene catalyzed by palladium. *J. Am. Chem. Soc.* **2005**, *127*, 17888−17893.
(28) Lyngvi, E.; Sanhueza, I. A.; Schoenebeck, F. Dispersion Makes the Difference: Bisligated Transition States Found for the Oxidative Addition of Pd(PtBu3)2 to Ar-OSO2R and Dispersion Controlled Chemoselectivity in Reactions with Pd[P(iPr)(tBu2)]2. *Organometallics* **2015**, *34*, 805−812.
(29) Qi, X.; Kohler, D. G.; Hull, K. L.; Liu, P. Energy Decomposition Analyses Reveal the Origins of Catalyst and Nucleophile Effects on Regioselectivity in Nucleopalladation of Alkenes. *J. Am. Chem. Soc.* **2019**, *141*, 11892−11904.
(30) Kohler, D. G.; Gockel, S. N.; Kennemur, J. L.; Waller, P. J.; Hull, K. L. Palladium-catalysed anti-Markovnikov selective oxidative amination. *Nat. Chem.* **2018**, *10*, 333−340.
(31) (a) Hegedus, L. S. *Transition Metals in the Synthesis of Complex Organic Molecules*; University Science Books: Mill Valley, 1994. (b) Negishi, E. *Organopalladium Chemistry for Organic Synthesis*; Wiley: New York, 2002; Vol. 2, p 2119.
(32) (a) Semmelhack, M. F.; Bodurow, C. Intramolecular alkoxypalladation/carbonylation of alkenes. *J. Am. Chem. Soc.* **1984**, *106*, 1496−1498. (b) Hayashi, T.; Yamasaki, K.; Mimura, M.; Uozumi, Y. Deuterium-Labeling Studies Establishing Stereochemistry at the Oxypalladation Step in Wacker-Type Oxidative Cyclization of an o-Allylphenol. *J. Am. Chem. Soc.* **2004**, *126*, 3036−3037. (c) Ward, A. F.; Xu, Y.; Wolfe, J. P. Synthesis of chromans via Pd-catalyzed alkene carboetherification reactions. *Chem. Commun.* **2012**, *48*, 609−611.
(33) (a) Isomura, K.; Okada, N.; Saruwatari, M.; Yamasaki, H.; Taniguchi, H. Firm evidence for cis-aminopalladation in the reactions of 1-aminohexatrienes with palladium dichloride. *Chem. Lett.* **1985**, *14*, 385−388. (b) Ye, X.; White, P. B.; Stahl, S. S. Mechanistic Studies of Wacker-Type Amidocyclization of Alkenes Catalyzed by (IMes)-Pd(TFA)2(H2O): Kinetic and Stereochemical Implications of Proton Transfer. *J. Org. Chem.* **2013**, *78*, 2083−2090. (c) Weinstein, A. B.; Stahl, S. S. Reconciling the Stereochemical Course of Nucleopalladiation with the Development of Enantioselective Wacker-Type Cyclizations. *Angew. Chem., Int. Ed.* **2012**, *51*, 11505−11509.
(34) (a) Babij, N. R.; Boothe, J. R.; McKenna, G. M.; Fornwald, R. M.; Wolfe, J. P. Stereocontrolled synthesis of bicyclic ureas and sulfamides via Pd-catalyzed alkene carboamination reactions. *Tetrahedron* **2019**, *75*, 4228−4243. (b) Hinds, E. M.; Wolfe, J. P. A Cross-Metathesis/Aza-Michael Reaction Strategy for the Synthesis of Cyclic and Bicyclic Ureas. *J. Org. Chem.* **2018**, *83*, 10668−10676. (c) White, D. R.; Herman, M. I.; Wolfe, J. P. Palladium-Catalyzed Alkene Carboalkoxylation Reactions of Phenols and Alcohols for the Synthesis of Carbocycles. *Org. Lett.* **2017**, *19*, 4311−4314.
(35) (a) Weinstein, A. B.; Schuman, D. P.; Tan, Z. X.; Stahl, S. S. Synthesis of Vicinal Aminoalcohols by Stereoselective Aza-Wacker Cyclizations: Access to (−)-Acosamine by Redox Relay. *Angew. Chem., Int. Ed.* **2013**, *52*, 11867−11870. (b) Redford, J. E.; McDonald, R. I.; Rigsby, M. L.; Wiensch, J. D.; Stahl, S. S. Stereoselective Synthesis of cis-2,5-Disubstituted Pyrrolidines via Wacker-Type Aerobic Oxidative Cyclization of Alkenes with tert-Butanesulfinamide Nucleophiles. *Org. Lett.* **2012**, *14*, 1242−1245. (c) McDonald, R. I.; Stahl, S. S. Modular Synthesis of 1,2-Diamine Derivatives by Palladium-Catalyzed Aerobic Oxidative Cyclization of Allylic Sulfamides. *Angew. Chem., Int. Ed.* **2010**, *49*, 5529−5532.

https://dx.doi.org/10.1021/acs.joc.0c02777
J. Org. Chem. 2021, 86, 3923−3942

(36) (a) Tamaru, Y.; Hojo, M.; Yoshida, Z. Inter- and intramolecular di-alkoxycarbonylation of 3-butenols catalyzed by palladium(II). *Tetrahedron Lett.* **1987**, *28*, 325−328. (b) Tamaru, Y.; Hojo, M.; Yoshida, Z. Palladium(II)-catalyzed carbonylation of 3-buten-1-ols and 3-butyn-1-ols: an efficient synthesis of. gamma.-butyrolactones. *J. Org. Chem.* **1991**, *56*, 1099−1105. (c) Ferguson, J.; Zeng, F.; Alper, H. Synthesis of Coumarins via Pd-Catalyzed Oxidative Cyclocarbonylation of 2-Vinylphenols. *Org. Lett.* **2012**, *14*, 5602−5605.

(37) (a) Andersson, P. G.; Bäckvall, J.-E. C-O and C-N Bond Formation Involving Conjugated Dienes and Allylpalladium Intermediates. In *Handbook of Organopalladium Chemistry for Organic Synthesis*; Negish, E.-i., Ed.; Wiley: New York, 2002; pp 1859−1874. (b) Bäckvall, J.-E.; Granberg, K. L.; Andersson, P. G.; Gatti, R.; Gogoll, A. Stereocontrolled lactonization reactions via palladium-catalyzed 1,4-addition to conjugated dienes. *J. Org. Chem.* **1993**, *58* (20), 5445−5451. (c) Bäckvall, J.-E.; Bystrom, S. E.; Nordberg, R. E. Stereo- and regioselective palladium-catalyzed 1,4-diacetoxylation of 1,3-dienes. *J. Org. Chem.* **1984**, *49*, 4619−4631. (d) Bäckvall, J.-E.; Nordberg, R. E.; Wilhelm, D. Dual stereoselectivity in the nucleophilic attack on (π-allyl)palladium complexes. *J. Am. Chem. Soc.* **1981**, *107*, 6892−6898.

(38) Trend, R. M.; Ramtohul, Y. K.; Stoltz, B. M. Oxidative Cyclizations in a Nonpolar Solvent Using Molecular Oxygen and Studies on the Stereochemistry of Oxypalladation. *J. Am. Chem. Soc.* **2005**, *127*, 17778−17788.

(39) Nielsen, R. J.; Keith, J. M.; Stoltz, B. M.; Goddard, W. A. A Computational Model Relating Structure and Reactivity in Enantioselective Oxidations of Secondary Alcohols by (−)-Sparteine-PdII Complexes. *J. Am. Chem. Soc.* **2004**, *126*, 7967−7974.

(40) (a) Brooks, J. L.; Xu, L.; Wiest, O.; Tan, D. S. Diastereoselective Synthesis of Highly Substituted Tetrahydrofurans by Pd-Catalyzed Tandem Oxidative Cyclization-Redox Relay Reactions Controlled by Intramolecular Hydrogen Bonding. *J. Org. Chem.* **2017**, *82*, 57−75. (b) Ammann, S. E.; Rice, G. T.; White, M. C. Terminal Olefins to Chromans, Isochromans, and Pyrans via Allylic C-H Oxidation. *J. Am. Chem. Soc.* **2014**, *136*, 10834−10837. (c) Ghebreghiorgis, T.; Kirk, B. H.; Aponick, A.; Ess, D. H. Multiple Mechanisms in Pd(II)-Catalyzed Sn2′ Reactions of Allylic Alcohols. *J. Org. Chem.* **2013**, *78*, 7664−7673. (d) Jensen, K. H.; Webb, J. D.; Sigman, M. S. Advancing the Mechanistic Understanding of an Enantioselective Palladium-Catalyzed Alkene Difunctionalization Reaction. *J. Am. Chem. Soc.* **2010**, *132*, 17471−17482.

(41) Baldwin, J. E. Rules for Ring Closure. *J. Chem. Soc., Chem. Commun.* **1976**, *18*, 734−736.

(42) Kočovský, P.; Bäckvall, J. E. The syn/anti-dichotomy in the palladium catalyzed addition of nucleophiles to alkenes. *Chem. - Eur. J.* **2015**, *21*, 36−56.

(43) Kozuch, S.; Shaik, S. A Combined Kinetic-Quantum Mechanical Model for Assessment of Catalytic Cycles: Application to Cross-Coupling and Heck Reactions. *J. Am. Chem. Soc.* **2006**, *128*, 3355−3365.

(44) (a) Engelin, C.; Jensen, T.; Rodriguez-Rodriguez, S.; Fristrup, P. Mechanistic Investigation of Palladium-Catalyzed Allylic C-H Activation. *ACS Catal.* **2013**, *3*, 294−302. (b) Simmons, E. M.; Hartwig, J. F. On the Interpretation of Deuterium Kinetic Isotope Effects in C-H Bond Functionalizations by Transition-Metal Complexes. *Angew. Chem., Int. Ed.* **2012**, *51*, 3066−3072.

(45) (a) Guo, J.-Y.; Minko, Y.; Santiago, C. B.; Sigman, M. S. Developing Comprehensive Computational Parameter Sets To Describe the Performance of Pyridine-Oxazoline and Related Ligands. *ACS Catal.* **2017**, *7*, 4144−XXX. (b) Santiago, C. B.; Guo, J.-Y.; Sigman, M. S. Predictive and mechanistic multivariate linear regression models for reaction development. *Chem. Sci.* **2018**, *9*, 2398−XXXX. (c) Ferreira, M. A. B.; De Jesus Silva, J.; Grosslight, S.; Fedorov, A.; Sigman, M. S.; Coperet, C. Non-Covalent Interactions Drive the Efficiency of Molybdenum Imido Alkylidene Catalysts for Olefin Metathesis. *J. Am. Chem. Soc.* **2019**, *141*, 10788−10800. (d) De Jesus Silva, J.; Ferreira, M. A. B.; Fedorov, A.; Sigman, M. S.; Coperet, C. Molecular-level insight in supported olefin metathesis catalysts by combining surface organometallic chemistry, high throughput experimentation, and data analysis. *Chem. Sci.* **2020**, *11*, 6717−6723.

(46) (a) Santiago, C. B.; Milo, A.; Sigman, M. S. Developing a Modern Approach To Account for Steric Effects in Hammett-Type Correlations. *J. Am. Chem. Soc.* **2016**, *138*, 13424. (b) Hollingsworth, C. A.; Seybold, P. G.; Hadad, C. M. Substituent effects on the electronic structure and pKa of benzoic acid. *Int. J. Quantum Chem.* **2002**, *90*, 1396.

(47) Verloop, A. In *Drug Design*; Ariens, E. J., Ed.; Academic Press, 1976; Vol. 3, pp 133−187.

(48) Perrin, D. D.; Armarego, W. L. F.; Perrin, D. R. In *Purification of laboratory chemicals*; Oxford, Pergamon Press: New York, 1966; 1st Edition.

(49) Kalaitzakis, D.; Rozzell, J. D.; Smonou, I. K. Synthesis of Valuable Chiral Intermediates by Isolated Ketoreductases: Application in the Synthesis of α-Alkyl-β-hydroxy Ketones and 1,3-Diols. *Adv. Synth. Catal.* **2006**, *348*, 1958−1969.

(50) Kondaiah, G. C. M.; Reddy, L. A.; Babu, K. S.; Gurav, V. M.; Huge, K. G.; Bandichhor, R.; Reddy, P. P.; Bhattacharya, A.; Anand, R. V. Boric acid: an efficient and environmentally benign catalyst for transesterification of ethyl acetoacetate. *Tetrahedron Lett.* **2008**, *49*, 106−109.

(51) Gohain, M.; Kumar, V.; Van Tonder, J. H.; Swart, H. C.; Ntwaeabowa, O. M.; Bezuidenhoudt, B. C. B. Nano CuFe2O4: an efficient, magnetically separable catalyst for transesterification of β-ketoesters. *RSC Adv.* **2015**, *5*, 18972−18976.

(52) Parveen, N.; Saha, R.; Sekar, G. Stable and Reusable Palladium Nanoparticles-Catalyzed Conjugate Addition of Aryl Iodides to Enones: Route to Reductive Heck Products. *Adv. Synth. Catal.* **2017**, *359*, 3741−3751.

(53) Gładkowski, W.; Skrobiszewski, A.; Mazur, M.; Siepka, M.; Pawlak, A.; Obminska-Mrukowicz, B.; Białonska, A.; Poradowski, D.; Drynda, A.; Urbaniak, M. Synthesis and anticancer activity of novel halolactones with β-aryl substituents from simple aromatic aldehydes. *Tetrahedron* **2013**, *69*, 10414−10423.

(54) Bowie, J. H.; Eichinger, P. C. H. J. *Org. Mass Spectrom.* **1987**, *22*, 103−108.

(55) Frisch, M. J.; Trucks, G. W.; Schlegel, H. B.; Scuseria, G. E.; Robb, M. A.; Cheeseman, J. R.; Scalmani, G.; Barone, V.; Petersson, G. A.; Nakatsuji, H.; Li, X.; Caricato, M.; Marenich, A. V; Bloino, J.; Janesko, B. G.; Gomperts, R.; Mennucci, B.; Hratchian, H. P.; Ortiz, J. V; Izmaylov, A. F.; Sonnenberg, J. L.; Williams Ding, F.; Lipparini, F.; Egidi, F.; Goings, J.; Peng, B.; Petrone, A.; Henderson, T.; Ranasinghe, D.; Zakrzewski, V. G.; Gao, J.; Rega, N.; Zheng, G.; Liang, W.; Hada, M.; Ehara, M.; Toyota, K.; Fukuda, R.; Hasegawa, J.; Ishida, M.; Nakajima, T.; Honda, Y.; Kitao, O.; Nakai, H.; Vreven, T.; Throssell, K.; Montgomery, J. A., Jr.; Peralta, J. E.; Ogliaro, F.; Bearpark, M. J.; Heyd, J. J.; Brothers, E. N.; Kudin, K. N.; Staroverov, V. N.; Keith, T. A.; Kobayashi, R.; Normand, J.; Raghavachari, K.; Rendell, A. P.; Burant, J. C.; Iyengar, S. S.; Tomasi, J.; Cossi, M.; Millam, J. M.; Klene, M.; Adamo, C.; Cammi, R.; Ochterski, J. W.; Martin, R. L.; Morokuma, K.; Farkas, O.; Foresman, J. B.; Fox, D. J. *Gaussian 16 Rev. C.01.*; Gaussian, Inc.: Wallingford, CT, 2016.

(56) Zhao, Y.; Truhlar, D. G. The M06 Suite of Density Functionals for Main Group Thermochemistry, Thermochemical Kinetics, Noncovalent Interactions, Excited States, and Transition Elements: Two New Functionals and Systematic Testing of Four M06-Class Functionals and 12 Other Function. *Theor. Chem. Acc.* **2008**, *120*, 215−241.

(57) (a) Weigend, F.; Ahlrichs, R. Balanced Basis Sets of Split Valence, Triple Zeta Valence and Quadruple Zeta Valence Quality for H to Rn: Design and Assessment of Accuracy. *Phys. Chem. Chem. Phys.* **2005**, *7*, 3297−3305. (b) Weigend, F. Accurate Coulomb-Fitting Basis Sets for H to Rn. *Phys. Chem. Chem. Phys.* **2006**, *8*, 1057−1065.

(58) (a) Krishnan, R.; Binkley, J. S.; Seeger, R.; Pople, J. A. Self-Consistent Molecular Orbital Methods. XX. A Basis Set for Correlated Wave Functions. *J. Chem. Phys.* **1980**, *72*, 650−654.

https://dx.doi.org/10.1021/acs.joc.0c02777
J. Org. Chem. 2021, 86, 3923−3942

(b) McLean, A. D.; Chandler, G. S. Contracted Gaussian Basis Sets for Molecular Calculations. I. Second Row Atoms, Z = 11−18. *J. Chem. Phys.* **1980**, *72*, 5639−5648.
(59) *Maestro*, version 9.6; Schrödinger, LLC, New York, NY.
(60) Dennington, R.; Keith, T.; Millam, J. *GaussView*, version 5; Semichem, Inc., Shawnee Mission, KS. 2009.
(61) Legault, C. Y. *CYLview version 20*; Université de Sherbrooke: Quebéc, 2020.
(62) Sweeney, J. B.; Ball, A. K.; Smith, L. J. Catalytic C-C Bond Formation Using a Simple Nickel Precatalyst System: Base- and Activator-Free Direct C-Allylation by Alcohols and Amines. *Chem. - Eur. J.* **2018**, *24*, 7354−7357.
(63) King, J. F.; Rathore, R.; Lam, J. Y. L.; Guo, Z. R.; Klassen, D. F. pH optimization of nucleophilic reactions in water. *J. Am. Chem. Soc.* **1992**, *114*, 3028−3033.
(64) Murphy, P. V.; O'Sullivan, T. J.; Kennedy, B. D.; Geraghty, N. W. A. The reactions of diazo compounds with lactones. Part 2. The reaction of cyclic 2-diazo-1,3-dicarbonyl compounds with diketene: benzofuran formation. *J. Chem. Soc., Perkin Trans. 1* **2000**, 2121−2126.
(65) Šmit, B. M.; Pavlovic, R. Z. Three-step synthetic pathway to fused bicyclic hydantoins involving a selenocyclization step. *Tetrahedron* **2015**, *71*, 1101−1108.
(66) Mori, K.; Mitsui, T.; Fukami, J.; Ohtaki, T. Synthesis of Compounds with Juvenile Hormone Activity Part VII. A Convenient Non-stereoselective Synthesis of the C18-Cecropia Juvenile Hormone and its Analogues; Effect of the Terminal Alkyl Substituents on Biological Activity. *Agric. Biol. Chem.* **1971**, *35*, 1116−1127.
(67) Imagawa, H.; Kurisaki, T.; Nishizawa, M. Mercuric Triflate-Catalyzed Synthesis of 2-Methylfurans from 1-Alkyn-5-ones. *Org. Lett.* **2004**, *6*, 3679−3681.
(68) Chen, P.; Meng, Y.; Yang, Q.; Wu, J.; Xiao, Y.; Gorja, D. R.; Song, C.; Chang, J. Selective synthesis of 2,5-disubstituted furan-3-carboxylates and the isomeric 2,4-disubstituted furan-3-carboxylates. *RSC Adv.* **2015**, *5*, 79906−79914.
(69) Tsuji, H.; Yamagata, K.-I.; Ueda, Y.; Nakamura, E. Indium-Catalyzed Synthesis of Furans and Pyrroles via Cyclization of α-Propargyl-β-keto Esters. *Synlett* **2011**, 1015−1017.
(70) Noda, H.; Motokura, K.; Miyaji, A.; Baba, T. Efficient Allylation of Nucleophiles Catalyzed by a Bifunctional Heterogeneous Palladium Complex-Tertiary Amine System. *Adv. Synth. Catal.* **2013**, *355*, 973−980.
(71) Yang, N. Y.; Li, Z. L.; Ye, L.; Tana, B.; Liu, X. Y. Organic base-catalysed solvent-tuned chemoselective carbotrifluoromethylation and oxytrifluoromethylation of unactivated alkenes. *Chem. Commun.* **2016**, *52*, 9052−9055.
(72) Deschamp, J.; Riant, O. Efficient Construction of Polycyclic Derivatives via a Highly Selective CuI-Catalyzed Domino Reductive-Aldol Cyclization. *Org. Lett.* **2009**, *11*, 1217−1220.
(73) Tang, E.; Huang, X.; Xu, W.-M. Polymer-supported selenium-induced electrophilic cyclization: solid-phase synthesis of poly-substituted dihydrofurans and tetrahydrofurans. *Tetrahedron* **2004**, *60*, 9963−9969.
(74) Senthilkumar, S.; Thangapriya, C.; Alagumurugayee, R.; Kumarraja, M. MMZNiY-Catalyzed Tsuji-Trost Type of Reaction: A Selective Mono/Bis Allylation of Dicarbonyl Compounds. *Catal. Lett.* **2017**, *147*, 2755−2763.

https://dx.doi.org/10.1021/acs.joc.0c02777
J. Org. Chem. 2021, 86, 3923−3942